



FAKULTÄT FÜR  
NATURWISSENSCHAFTEN

# **Structural and Functional Brain Changes after a 40-days short-term Mindfulness Meditation Training**

**PhD Thesis**

for the degree of

**doctor rerum naturalium**

**(Dr. rer. nat.)**

approved by the Faculty of Natural Sciences of Otto von  
Guericke University Magdeburg

by Chuan-Chih Yang M.Sc.

born on 06.02.1983 in Taichung, Taiwan

Examiner: Prof. Dr. med. Martin Walter

Prof. Dr. Anke Karl

submitted on: 29.01.2020

defended on: 21.09.2020

”May all beings have happy minds.”

*The Buddha, Karaniya Metta Sutta*

## ABSTRACT

The objective of the current thesis was to study the functional and structural brain changes after a 40 days short-term mindfulness meditation training in meditation-naive subjects. In this thesis, both modalities- functional and structural imaging analysis were used to investigate the longitudinal brain changes related to mindfulness meditation training, further it was put into the framework of potentially changing depression symptom and anxiety by using behavioral questionnaires.

An increasing number of neuroimaging studies showed that mindfulness meditation is associated with different functional and structural configurations of the default mode network (DMN), salience network (SN), executive network at resting-state. In the first part of the study, I compared the brain network functional connectivity differences between rest and meditation by utilizing the resting-state functional connectivity methods. Further, I also applied the Regional Homogeneity approach to investigate the local differences. Significant differences in functional connectivity both between states (rest vs. meditation) and between timepoints (pre- vs. post- training) was observed. The internal consistency of the functional activity at the precuneus and the temporo-parietal junction increased during meditation, while the decreased pattern at the frontal brain areas was observed. In addition, I analyzed the regional connectivity of the dorsal anterior cingulate cortex (dACC), and observed the connectivity with anterior insula (AI) during meditation state was reduced. I further discovered that the resting-state functional connectivity between the pregenual anterior cingulate (pgACC) and dorsal medial prefrontal cortex (dmPFC) was reduced after the training of mindfulness meditation. Of note, I observed significant reduction of the depression/anxiety scores. In the second part of the study, the increase of cortical thickness and the reduction of low-frequency amplitudes (ALFF) was observed in precuneus, which is a posterior DMN region, that both the structural and functional effects were seen due to mindfulness meditation training. Further, the reduction of ALFF in left precuneus/posterior

cingulate cortex (PCC) is related with the decrease of the depression scores.

In summary, mindfulness meditation leads to plasticity-related network alteration in brain areas that are affected by mood disorders such as depression, which might be of therapeutic benefit.

## ZUSAMMENFASSUNG

Ziel der vorliegenden Arbeit war es, in Folge eines 40-tägigen Achtsamkeitsmeditationstraining Veränderungen in den Gehirnen von Probanden, die zuvor noch nie meditiert hatten, zu untersuchen. In dieser Arbeit wurden die Modalitäten funktionelle und strukturelle Bildgebung verwendet, um die langfristigen Veränderungen des Gehirns im Zusammenhang mit Achtsamkeitsmeditationstraining zu untersuchen. Zusätzlich wurden diese mithilfe von Fragebögen zum Verhalten erfasst und im Kontext potenziell veränderter Depressionssymptomatik und angst analysiert.

Eine wachsende Anzahl von Studien im Bereich der funktionellen Bildgebung haben gezeigt, dass Achtsamkeitsmeditation mit verschiedenen funktionellen und strukturellen Konfigurationen der sogenannten Default-Mode Netzwerkes (DMN), des Salienz-Netzwerkes (SN) und des Exekutiv-Netzwerkes zusammenhängt. Im ersten Teil der Studie verglichen wir Unterschiede in der Netzwerkkonnektivität zwischen Ruhe und während der Meditation unter Verwendung üblicher Methoden zur Analyse funktioneller Konnektivität im Ruhezustand. Interregionale Methoden wurden lokalen Maßen, wie der regionalen Homogenität, gegenübergestellt. Wie erwartet wurden signifikante Unterschiede in der funktionellen Konnektivität sowohl zwischen den Zuständen (Ruhe versus Meditation) als auch zwischen den Zeitpunkten (vor versus nach dem Training) beobachtet. Während der Meditation nahm die innere Konsistenz im Precuneus und im temporo-parietalen Übergang zu, während die innere Konsistenz der frontalen Hirnregionen abnahm. Eine weiterführende Analyse der regionalen Konnektivität des dorsalen anterioren cingulären Kortex ergab eine verminderte Konnektivität mit der anterioren Insula während der Meditation. Nach Abschluss des Meditationstrainings wurde eine verminderte funktionelle Konnektivität im Ruhezustand zwischen dem pregenualen anterioren cingulären und dem dorsalen präfrontalen Kortex beobachtet. Eine wichtige Beobachtung war, dass nach dem Meditationstraining signifikant verringerte Depressions- / Angstwerte beobachtet wurden. Im zweiten Teil der

Studie fanden wir überlappende strukturelle und funktionelle Effekte in Precuneus. In dieser Region des posterioren DMN, nahm die kortikale Dicke zu und die niederfrequenten Amplituden (ALFF) nahmen ab, während die Abnahme von ALFF im linken Precuneus/posterioren Cingulum mit der Reduktion von Depressionswerten (CES-D) korrelierte.

Zusammenfassend lässt sich sagen, dass Achtsamkeitsmeditation von therapeutischem Nutzen sein könnte, indem sie plastizitätsbedingte Netzweränderungen in Arealen induziert, die bei affektiven Störungen, wie Depressionen, verändert sind.

## TABLE OF CONTENTS

<b>List of Tables</b> . . . . .	xi
<b>List of Figures</b> . . . . .	xii
<b>List of Abbreviations</b> . . . . .	xv
<b>Chapter 1: Introduction</b> . . . . .	1
1.1 Mindfulness Meditation . . . . .	1
1.1.1 Historical Origin . . . . .	2
1.2 Neuroplasticity . . . . .	2
1.3 Resting-state fMRI . . . . .	4
1.3.1 Background . . . . .	4
1.3.2 Brain Network . . . . .	4
1.4 Structural MRI . . . . .	5
1.5 Mindfulness Meditation in fMRI studies . . . . .	6
1.5.1 Background . . . . .	6
1.5.2 Previous Studies . . . . .	7
1.6 Mindfulness Meditation Intervention for Depression . . . . .	11

1.6.1	Clinical Evidence . . . . .	11
1.6.2	Clinical Rational . . . . .	11
1.6.3	Mechanistic Evidence . . . . .	12
1.7	Specific Aim of the Thesis . . . . .	13
1.7.1	Aims on Multi-modality . . . . .	14
1.7.2	Hypotheses . . . . .	14
<b>Chapter 2: General Methods . . . . .</b>		<b>15</b>
2.1	Subjects . . . . .	15
2.2	Mindfulness Meditation Study Details . . . . .	15
2.2.1	Study Design . . . . .	15
2.2.2	Mindfulness Meditation Training . . . . .	16
2.3	Self-report Measures . . . . .	18
2.4	Data Details . . . . .	19
2.4.1	Data Acquisition . . . . .	19
2.4.2	MR Sequence Parameters . . . . .	19
2.4.3	Data Preprocessing . . . . .	20
2.5	Brain Function - Resting-state fMRI (rs-fMRI) Analysis . . . . .	21
2.5.1	Functional Connectivity (FC) Analysis . . . . .	21
2.5.2	ReHo Analysis . . . . .	24
2.5.3	ALFF Analysis . . . . .	24
2.6	Brain Structure - Structural Magnetic Resonance Imaging . . . . .	26
2.6.1	Cortical Thickness . . . . .	26



2.6.2	Subcortical Volume . . . . .	27
2.7	Statistical Analysis . . . . .	28
2.7.1	Behavioural Data Analysis . . . . .	28
2.7.2	Seed-based FC Analysis . . . . .	28
2.7.3	Group ICA . . . . .	28
2.7.4	ALFF Analysis . . . . .	28
2.7.5	Cortical Thickness Analysis . . . . .	29
2.7.6	Subcortical Volume Analysis . . . . .	29
2.7.7	Post-hoc Correlation Analysis . . . . .	29
<b>Chapter 3:</b>	<b>Results . . . . .</b>	<b>31</b>
3.1	Subject Demographic . . . . .	31
3.2	Results of Behavioral Self-report Measures . . . . .	32
3.2.1	Behavioral Self-report Measures . . . . .	32
3.3	Brain Function - Functional Brain Imaging Results . . . . .	32
3.3.1	Seed-based FC . . . . .	33
3.3.2	Group ICA . . . . .	36
3.3.3	ReHo . . . . .	37
3.3.4	ALFF . . . . .	37
3.4	Brain Structure - Structural Brain Imaging Results . . . . .	38
3.4.1	Cortical Thickness . . . . .	38
3.4.2	Subcortical Volume . . . . .	39
<b>Chapter 4:</b>	<b>General Discussion . . . . .</b>	<b>50</b>

4.0.1	Summary of Findings across Modalities . . . . .	50
4.1	Discussion . . . . .	51
4.1.1	Discussion Clinical . . . . .	51
4.1.2	Discussion - Functional Brain Imaging Results . . . . .	52
4.1.3	Discussion - ALFF and Structural Brain Imaging Results . . . . .	55
4.1.4	Discussion of Combination of Results from rs-fMRI / Structural MRI / Clinical . . . . .	58
<b>Chapter 5: Conclusion . . . . .</b>		<b>62</b>
5.0.1	Summary . . . . .	62
5.0.2	Limitations . . . . .	63
<b>Appendix A: Data Processing . . . . .</b>		<b>67</b>
A.1	ALFF analysis (with no scrubbing) . . . . .	67
A.2	Statistical Analysis . . . . .	67
<b>Appendix B: ALFF Results . . . . .</b>		<b>69</b>
B.1	The whole brain ALFF analysis result: ALFF changes after 40-days mind- fulness meditation training . . . . .	69
B.2	Post hoc correlation analysis results . . . . .	69
<b>References . . . . .</b>		<b>83</b>
<b>Publikationsliste . . . . .</b>		<b>84</b>

**Erklärung zur strafrechtlichen Verurteilung . . . . . 85**

**Ehrenerklärung . . . . . 86**

## LIST OF TABLES

3.1	Subject demographic and exploratory behavioural measures. Group mean and standard deviation are listed [1]. . . . .	31
3.2	Primary behavioural outcome . . . . .	32
3.3	Exploratory behavioural measures (n=14) [1] . . . . .	33
3.4	Regions showing functional differences between conditions (rest versus meditation [2]) . . . . .	40
3.5	Regions showing RSFC differences between time points [2] . . . . .	41
3.6	Summary of differences in subcortical volumes (mm <sup>3</sup> ) of 16 brain regions between timepoints . . . . .	49

## LIST OF FIGURES

1.1	Schematic representation of the growth of awareness described in yoga texts <sup>1</sup>	3
1.2	Resting state functional connectivity reveals correlations and anticorrelations with the default mode network <sup>3</sup> . . . . .	6
1.3	Mindfulness Meditation studies using resting-state fMRI . . . . .	8
1.4	Mindfulness Meditation studies using structural MRI . . . . .	9
1.5	Mindfulness Meditation studies using resting-state fMRI and structural MRI	10
2.1	Study design- longitudinal MR imaging acquisition. At day 0 (TP1), I only acquired resting-state fMRI scans and structural MRI scans. While at day 40 (TP2) and day 90 (TP3), in addition to these two scans I acquired meditation scan, in which the subjects performed meditation while I ran the Echo-planar imaging (EPI) sequence . . . . .	16
2.2	8-week mindfulness meditation training course (on site training + minimum 10 minutes daily home practice), which includes simple physical and breathing exercises and Vipassana meditation exercises . . . . .	17
2.3	Seed ROIs used for RSFC analysis. ROI1: pregenual ACC (pgACC) as marked in red color. ROI2: dorsal ACC (dACC) as marked in blue color overlaid on the T1 anatomical MNI space [2] . . . . .	22
3.1	Paired comparison of seed-based FC maps (seed = pgACC) between rest and meditation at TP2 ( $p < 0.05$ , FWE-corrected). Bar plot represents the t-values. White labels indicate the coordinate of each slice in the MNI frame of reference (x, z). [2] . . . . .	34
3.2	Paired comparison of seed-based FC maps (seed = dACC) between rest and meditation at TP2. FC decreases between dorsal ACC and left AI during meditation as compared to rest ( $p < 0.05$ , FWE-corrected). Bar plot represents the t-values. White labels indicate the coordinate of each slice in the MNI frame of reference (x, z) [2]. . . . .	35

3.3	Longitudinal seed-based RSFC results (seed = pgACC). ( $p < 0.05$ , FWE-corrected). Bar plot represents the t-values. White labels indicate the coordinate of each slice in the MNI frame of reference (x, z) [2] . . . . .	42
3.4	Longitudinal seed-based RSFC results (seed = dACC). ( $p < 0.05$ , FWE-corrected). Bar plot represents the t-values. White labels indicate the coordinate of each slice in the MNI frame of reference (x, z). [2] . . . . .	43
3.5	Mean power spectral density of the Default Mode Network (DMN) component. The peak power density was observed below 0.04 Hz for both conditions (Resting-State and Meditation-State). A.U. stands for arbitrary unit. [2] . . . . .	44
3.6	ICA results. DMN differences at TP2 for RS >MS and MS >RS ( $p < 0.05$ , FWE-corrected). Bar plot represents the t-values. White labels indicate the coordinate of each slice in the MNI frame of reference (x, z). [2] . . . . .	44
3.7	Regional homogeneity difference between MS and RS ( $p < 0.05$ , FWE-corrected). Bar plot represents the t-values. White labels indicate the coordinate of each slice in the MNI frame of reference (x, z). [2] . . . . .	45
3.8	Longitudinal ALFF decreases after mindfulness meditation training (TP1 >TP2): Left IPL (Left angular gyrus), left PCC/precuneus and right IPL (right supramarginal) were found (FDR corrected, $p < 0.05$ ). Colorbar shows the t-values. [1] . . . . .	45
3.9	Post-hoc correlation of mean ALFF at left PCC/precuneus with CES-D. Decreased ALFF at left PCC/precuneus was found positively correlated with the reduction of depression score (CES-D), $p = 0.024$ , $r = 0.619$ . [1] . . .	46
3.10	The STAI trait scores are negatively correlated with the percent thickness change in the left inferior temporal gyrus (Monte Carlo Simulation corrected. $p < 0.05$ ). $r = -0.86$ , $p = 0.001$ . Colorbar shows the false-positive rate ( $-\log_{10}(p)$ ): thresholds of -3, -1.3, 1.3, 3 correspond to p-values of -0.001, -0.05, 0.05, 0.001.[1] . . . . .	46

3.11	Whole brain pre-post cortical thickness changes (PC1: percent thickness change). Significant regional increases in cortical thickness following mindfulness meditation training in left precuneus (-12.7, -72.9, 40.7; shown in yellow) and left superior parietal lobule (-8.8, -89.2, 21.4; shown in red; $p < 0.05$ , corrected by Monte Carlo simulation). Colorbar shows the false-positive rate ( $-\log_{10}(p)$ ): thresholds of -3, -1.3, 1.3, 3 correspond to p-values of -0.001, -0.05, 0.05, 0.001. [1]	47
3.12	Subcortical volume differences before and after meditation training	48
4.1	Summary of main findings across modality	58
4.2	Longitudinal seed-based RSFC results (seed = pgACC) after 40 days of mindfulness meditation training ( $p < 0.05$ , FWE-corrected). A reduction of resting-state functional connectivity between pgACC and dmPFC, close to dorsal nexus region, was observed. [2]	60
4.3	Proposed hypothetical model of ketamine-associated changes in functional connectivity. In the healthy human brain, a single antidepressant dose of ketamine reduces functional connectivity of the dorsal nexus (DN) to the Default Mode Network (DMN; green)	61
B.1	Longitudinal ALFF decreased after mindfulness meditation training (TP1 Rest > TP2 Rest): Left IPL (left angular gyrus, -42, -60, 45; $t=5.97$ ), PCC/precuneus (6, -63, 27; $t=8.57$ ), middle temporal gyrus (-45, -60, 21; $t=9.34$ ) and MPFC (-9, 57, 27; $t=5.75$ ) were found. No correlations of behavioural scores were observed. [1]	69
B.2	The frame-wise displacement value (FD_Power) showed no significant difference between the time points ( $t=1.488$ , $p=0.162$ ) [1]	70
B.3	Head motion parameters, and the translation and rotation information and the FD values at TP1	71
B.4	Head motion parameters, and the translation and rotation information and the FD values at TP2 [1]	72

## Abbreviations

**AI** anterior insular

**ALFF** amplitude of low-frequency

**BOLD** blood-oxygen level dependent

**CEN** central executive network

**CES-D** Center for Epidemiologic Studies Depression Scale

**dACC** dorsal anterior cingulate cortex

**dIPFC** dorsolateral prefrontal cortex

**DMN** default mode network

**dmPFC** dorsal medial prefrontal cortex

**DN** dorsal nexus

**DPARSF** Data Processing Assistant for Resting-State fMRI

**EPI** echo-planar imaging

**FA** flip angle

**FDR** false discovery rate

**FFMQ** Five Facet Mindfulness Questionnaire

**FOV** field-of-view

**FWE** family-wise error

**FWHM** full-width-at-half-maximum

**GLM** general linear model

**HF-HRV** high-frequency heart rate variability

**IC** independent component

**ICA** independent component analysis

**IFG** inferior frontal gyrus

**IMBT** integrative body-mind training

**IPL** inferior parietal lobule

**LFFs** low frequency fluctuations



**lpPC** lateral posterior parietal cortex  
**MBI** mindfulness-based intervention  
**MBM** mindfulness-based meditation  
**MBSR** mindfulness-based stress reduction  
**MDD** major depressive disorder  
**MFC** medial frontal cortex  
**MP-RAGE** magnetization prepared rapid gradient-echo  
**MS** meditation state  
**PCC** posterior cingulate cortex  
**POMS** Profile of Mood States  
**RCT** randomised controlled trial  
**ReHo** regional homogeneity  
**RS** resting state  
**RSFC** resting state functional connectivities  
**rs-fMRI** resting-state functional Magnetic Resonance Imaging  
**RSNs** resting-state networks  
**SN** salience network  
**SPM** Statistical Parametric Mapping  
**TP1** time point 1  
**TP2** time point 2  
**TP3** time point 3  
**TPJ** temporo parietal junction  
**VBM** voxel-based morphometry  
**WHO** World Health Organization  
**YLD** lost to disability

# CHAPTER 1

## INTRODUCTION

The current thesis incorporates materials from the following papers: (1) Yang, C., Barrós-Loscertales, A., Li, M., Pinazo, D., Borchardt, V., Ávila, C., and Walter, M. Alterations in Brain Structure and Amplitude of Low-frequency after 8 weeks of Mindfulness Meditation Training in Meditation-Naïve Subjects. *Sci Rep* 9, 10977 (2019) [1]. (2) Yang, C., Barrós-Loscertales, A., Pinazo, D., Ventura-Campos, N., Borchardt, V., Bustamante, JC., Rodríguez-Pujadas, A., Fuentes-Claramonte, P., Balaguer, R., Ávila, C., and Walter, M. State and Training Effects of Mindfulness Meditation on Brain Networks Reflect Neuronal Mechanisms of Its Antidepressant Effect, *Neural Plasticity*, vol. 2016 [2]. In publication 1, the longitudinal structural brain changes of the participants after 40 days of mindfulness meditation training were investigated by using structural brain imaging modality. In publication 2, a longitudinal functional brain imaging study investigating the resting-state functional connectivities (RSFC) changes based on the same sample was carried out.

### 1.1 Mindfulness Meditation

There has been an increasing interest in Mindfulness meditation research in recent years. Mindfulness is a mental state achieved by attending to the present-moment awareness, while acknowledging one's feelings, bodily sensations and thoughts non-judgementally, which could be cultivated through meditation practice [3–5]. In recent western psychology, Mindfulness-based meditation (MBM) is increasingly being used to mitigate various mental and physical conditions, such as anxiety, depression, and drug addiction [6–10].

### 1.1.1 Historical Origin

The western practice of Mindfulness is based on Zen and modern Vipassana [11]. From Buddhism, Mindfulness involves the training of "sati". Sati is one of the seven factors of awakening in Buddhism, which according to Thomas William Rhys Davids, the British scholar of Pali language, who translated it into English, is literally 'memory', but was utilized respecting 'mindful and thoughtful' [12]. According to the description from yoga text, there are four mental states defined. Random thinking (cancalata), concentrative mind (ekagrata), focused meditation (dharana) and effortless meditation (dhyana) [13]. Mindfulness meditation is the closest to dhyana, the effortless meditation. In Figure 1.1, the schematic representation of the growth of awareness described in yoga texts are tabled.

## **1.2 Neuroplasticity**

Neuroplasticity, neuroelasticity, or neural plasticity, is the terminology to depict the brain changes which occur in response to acquired experience [14]. Neuroplasticity is observed at multiple scales, ranging from individual neurons alterations to cortical remapping [15]. Environmental input, behavior, emotions, and even thoughts may also lead to neuroplastic changes [15, 16]. When looking at the single cell level, synaptic plasticity means altered connections between neurons, while non-synaptic plasticity means changes in the intrinsic excitability. The Polish neuroscientist Jerzy Konorski was the first scientist to utilize the term neural plasticity [17]. When the term of neuroplasticity is applied to meditation, it is suggested that the mental training of meditation is similar to other types of skill acquisition which could induce brain plastic changes [14].





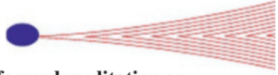
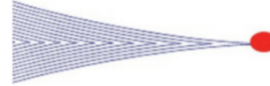


Growth of Awareness	Levels	States of Consciousness	Observation
	All Pervasive Awareness Unchanging	 <b>Kaivalya – Infinite Awareness/Consciousness</b>	Being one with Reality
	Higher States of Exposed Awareness	 <b>Higher Samadhi – 3D to All Pervasive Awareness</b>	Contained Quantum jumps to subtler & Causal Levels of the Subject
	Quantum Jump higher levels of Awareness	 <b>Samadhi: Merging Seer and Seen (Total 3D awareness)</b>	Identified into the object totally
	Exposed Attention Awareness	 <b>Defocused meditation or effortless meditation (<i>Dhyana</i>)</b>	Effortless single thought flow
	Focused Attention Awareness	 <b>Focused meditation (<i>Dharana</i>)</b>	One Object, One thought stream
	Channelized Attention	 <b>Non-meditative concentration (<i>Ekagrata</i>)</b>	One Subject and Multiple Thoughts
	Disturbed Attention	 <b>Random Thinking (<i>Canalata</i>)</b>	Multiple subjects underlined thoughts

Figure 1.1: Schematic representation of the growth of awareness described in yoga texts<sup>1</sup>

<sup>1</sup>Reproduced with permission from the corresponding author. Reprinted from "Evolution from four mental states to the highest state of consciousness: A neurophysiological basis of meditation as defined in yoga texts" by Deepeshwar et al. 2019, Meditation - Progress in brain research, volume 244, page 24, Copyright 2019 Elsevier

## 1.3 Resting-state fMRI

### 1.3.1 Background

Resting-state functional Magnetic Resonance Imaging (rs-fMRI) detects spontaneous low-frequency fluctuations (LFFs) signal to study the functional topology of the brain. Various Resting-state Networks (RSNs) or spatially distinct brain regions that show synchronous LFFs at rest has been identified by using this technique. Biswal was the first scientist discovered the technique in 1995 [18] and it was utilized extensively in various functional imaging studies for healthy and patient populations. Resting state functional connectivities (RSFC) methods is one of the methods being used to investigate the alteration of neural plasticity due to the training of mindfulness meditation practice. As Yang (2016) states, "The interregional dynamics of RSFC specifically afford the advantages of being task independent, rendering reliable estimates of neural circuit functionality corresponding to structural topography [19, 20]" [2]. Figure1.2 (reprinted from "The human brain is intrinsically organized into dynamic, anticorrelated functional networks" by Fox et al. 2005) shows two distinct brain networks when the participant is at rest.

### 1.3.2 Brain Network

As Yang (2019) states, "Increasing neuroimaging studies suggests that mindfulness meditation expertise is related to different functional and structural configurations of the default mode network (DMN), the salience network (SN) and the executive network at rest" [1]. The Salience Network (SN) is composed of the dorsal anterior cingulate cortex (dACC) and bilateral anterior insular. This network is associated with detecting and filtering salient stimuli and recruiting relevant functional networks [21]. It mediates the switch between the default mode network and central executive network [22]. The Central Executive Network (CEN) is composed of fronto-parietal areas, including dorsolateral prefrontal cortex (dlPFC) and lateral posterior parietal cortex (lpPC) [23]. CEN is concerned in high level

cognitive functions such as decision making, preserving and utilizing information in working memory, problem solving [24]. In depression, CEN deficiencies is often observed [25]. Since this network is very important for daily life activities, deterioration in activity like being decisive can be observed in subjects suffering from depression [26]. Further, cognitively demanding tasks which elicit activation in CEN have been consistently shown to elicit decreased activation in the default-mode network (DMN). As Yang (2016) states, "We know that the DMN involves several brain regions active when the brain is not actively engaged in a cognitively demanding task but rather is in a relaxed state [27]. Consistently, the DMN includes areas at the medial posterior cortex, specifically the posterior cingulate cortex (PCC; areas 23/31), the precuneus, and the medial frontal cortex (MFC, including areas 24/10-m/32), as well as bilateral inferior parietal and posterior temporal areas around the temporoparietal junction area (TPJ) [28]. To study the influence of mindfulness meditation practice on the neuronal level and its antidepressant effects, alteration in the activation pattern of the Default Mode Network (DMN) is of special interest and the DMN is therefore selected as the target brain network [29]" [2].

#### **1.4 Structural MRI**

According to Yang (2019), "To study brain morphometry, several methods have been proposed to investigate brain structural changes, such as voxel-based morphometry (VBM) [30] and the cortical thickness measure (Freesurfer)[31, 32]. The cortical thickness measure is preferred because it utilises brain geometry to conduct inter-subject registration, which contributes to a finer matching of homologous cortical locations than volumetric-based methods. Freesurfer is commonly applied in many cortical thickness studies [31, 33, 34], and in this study, Freesurfer is used for the cortical thickness analysis given its advantages over the volume-based morphometry method" [1].

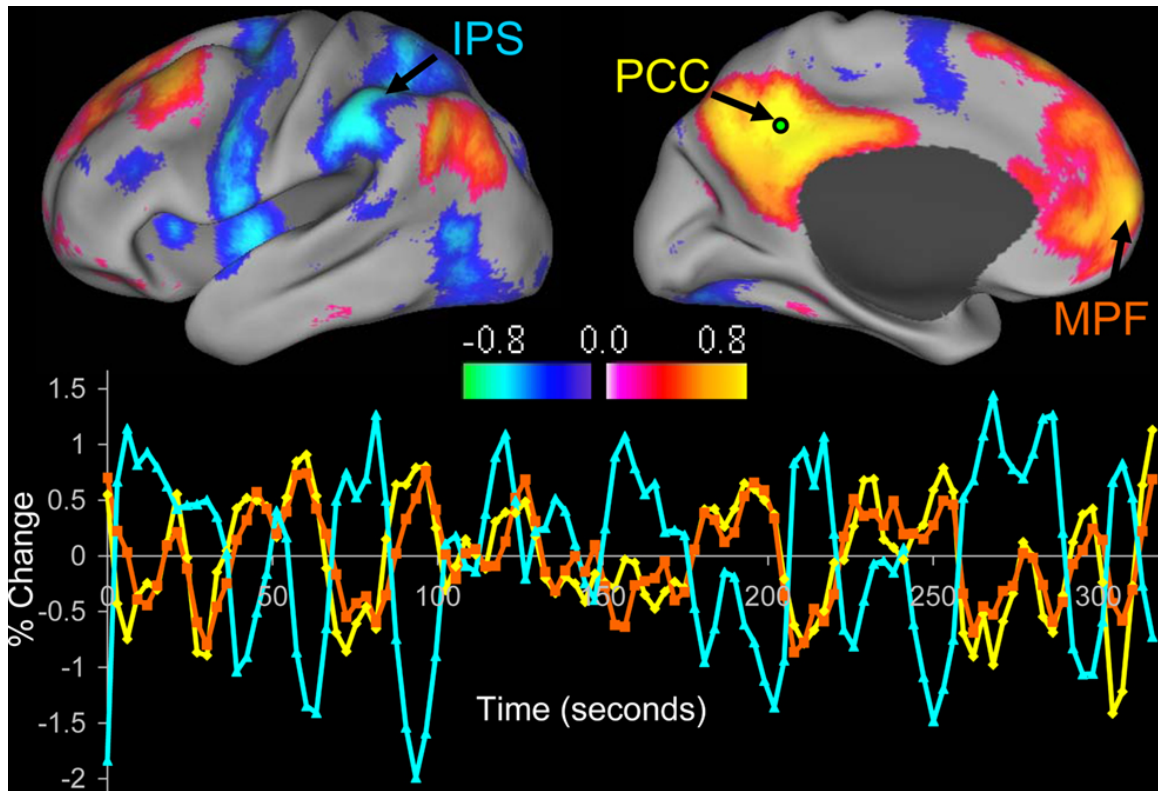


Figure 1.2: Resting state functional connectivity reveals correlations and anticorrelations with the default mode network. Correlations between a seed region in the posterior cingulate/precuneus (PCC) and all other voxels in the brain for a single subject during resting fixation. Both correlations (positive values) and anticorrelations (negative values) are shown, thresholded at  $R = 0.3$ .<sup>3</sup>

## 1.5 Mindfulness Meditation in fMRI studies

### 1.5.1 Background

The background information of the Mindfulness Meditation applied in functional neuroimaging research were fully introduced in [2]:

Despite the fact that recent neuroimaging studies indicate the several positive aspects of mindfulness practice, its neuronal mechanisms are still poorly understood. A main theme in meditation research is the question if the observed effects are dependent on prac-

<sup>3</sup>Reproduced from "The human brain is intrinsically organized into dynamic, anticorrelated functional networks" by Fox et al. 2005, PNAS, volume 102, issue 27, page 9673-9678. Copyright 2005 National Academy of Sciences

tice/expertise or on personal characteristics. Usually, studies on meditation compare expert practitioners with novice practitioners in cross-sectional studies [29, 35, 36]. Functional studies have employed fMRI block designs to investigate the blood-oxygen level dependent (BOLD) signal changes during meditation [35–37], as well as exploring resting state fMRI (rs-fMRI) differences between experienced meditators and novices [29, 35, 38]. Crucially, longitudinal studies of the impact of short-term meditation practice on the same novice group have the potential to reflect effects of meditation independently of individual differences, for example, personal interest in meditation or previous meditation experience. Hoelzel et al. [39] observed changes in gray matter density in a longitudinal study with 8 weeks of a mindfulness-based stress reduction (MBSR) programme.

As introduced in Yang (2019), "Brain research has yielded global and local levels of differences in brain activity and connectivity related to meditation affecting several brain regions involving the default mode network (DMN), the salience network and the executive network. It is noteworthy that global changes have shown reduced connectivity between the nodes of the DMN and other networks, as well as reduced local activity and connectivity of nodes within these networks (e.g., ReHo, ALFF, nodal strength)" [1]. As stated in Yang (2016), "To investigate the impact of mindfulness practice on the neuronal level and its antidepressant effects, alteration in the activation pattern of the Default Mode Network (DMN) is of particular interest and the DMN is thus selected as the target brain network[29]" [2].

### 1.5.2 Previous Studies

The relevant studies performed on investigating the mindfulness meditation and its neural correlates were introduced in [1]:

Previous studies have demonstrated the practice of mindfulness meditation leads to brain changes at either structural or functional levels [2, 33, 38, 40–43]. To track functional changes, resting-state functional magnetic resonance imaging (rs-fMRI) has been



Author (published year)	Modality	Study design	Group type	Duration of MM training	Longitudinal?	Subjects	Results
Creswell et al. 2016	Rs-fMRI (FC)	RCT	mindfulness meditation vs. relaxation training program	3 days	yes	Stressed job-seeking unemployed community adults	Mindfulness meditation training group increased posterior cingulate cortex rsFC with left dIPFC
Shao et al. 2016	Rs-fMRI (FC)	RCT	meditation vs. relaxation training	8 weeks	yes	healthy	Meditation vs relaxation training increased the positive connectivity between the PCC/precuneus and the pons, the direction of which was largely directed from the pons to the PCC/precuneus
Yang et al. 2016	Rs-fMRI (FC)	Cohort	No control group	40 days	yes	healthy	Reduced resting state functional connectivity between the pregenual anterior cingulate and dorsal medial prefrontal cortex was observed after MM training
Jang et al. 2018	Rs-fMRI (FC)	Cohort	35 Brain Wave Vibration meditation practitioners and 33 controls without previous meditation experience	(The meditation practitioners reported practicing BWV for more than 1 year (mean 39.9 months), control group has no previous experience)	no	healthy	Meditation practitioners showed significantly greater insula-related functional connectivity in the thalamus, caudate, middle frontal gyrus, and superior temporal gyrus than did controls
Kwak et al. 2019	Rs-fMRI (FC)	RCT	30 participants in meditation practice and 17 participants in a relaxation retreat	4 days	Yes (TP1,TP2,TP3)	healthy	Resting-state functional connectivity (rsFC) between the left rostral anterior cingulate cortex (rACC) and the dorsomedial prefrontal cortex (dmPFC), precuneus, and angular gyrus was significantly increased post-intervention in the meditation group compared with the relaxation group

Figure 1.3: Mindfulness Meditation studies using resting-state fMRI

proposed to analyse differential spontaneous modulations in the blood-oxygen-level dependent (BOLD) signal during resting conditions [19]. With rs-fMRI, researchers can characterise the brains spontaneous functional activities in terms of both brain network connectivity and local features, e.g. the amplitude of low-frequency fluctuations (ALFF) to characterise the amplitude of local spontaneous brain activity [44]. In contrast to the functional connectivity method, which measures the temporal synchronisation between brain areas, the ALFF method helps to localise the brain functional alterations [45]. The quantitative measurement of low-frequency oscillations, such as ALFF, provides promising tools to observe spontaneous BOLD signal alterations in regional activity. As such, it may offer insight into the direct local consequences of the previously reported structural changes. At structural level, Fox et al. reported and meta-analysed 123 brain structural differences using

Author (published year)	Modality	Study design	Group type	Duration of MM training	Longitudinal?	Subjects	Results
Santarnecci et al. 2014	Cortical thickness, subcortical volume	RCT	MBSR vs control	8 weeks	yes	healthy	Correlation between the increase in right insula thickness and the decrease in alexithymia levels during the MBSR training
Pickut et al. 2013	VBM	RCT	MBI (mindfulness-based intervention) vs UC (usual care)	8 weeks	yes	Parkinson's Disease (PD)	Increased GMD was found in the MBI compared to the UC group in the region of interest (ROI) analysis in the right amygdala, and bilaterally in the hippocampus
Tang et al. 2010	DTI (FA, fractional anisotropy)	RCT	IBMT(integrative body-mind training) vs RT (relaxation training)	11 hour	yes	Healthy undergraduate	Increases fractional anisotropy (FA), an index indicating the integrity and efficiency of white matter in the corona radiata
Hernández et al. 2016	VBM	Cohort	23 experienced practitioners of Sahaja Yoga Meditation and 23 non-meditators	(Meditators had between 5-26 years of experience (mean:14.1 SD (6.1) years)	no	healthy	Grey matter volume was larger in meditators relative to non-meditators across the whole brain

Figure 1.4: Mindfulness Meditation studies using structural MRI

several morphometric measures (e.g. cortical thickness, grey matter volume and concentration, fractional anisotropy, etc.) to show that mindfulness meditation also leads to significant brain structure changes [46]. Prior studies have pioneered longitudinal analysis on grey and white matter changes [47–49]. Tang et al. observed increased fractional anisotropy in the corona radiata connecting the cingulate cortex after an 11-hour integrative body-mind training (IBMT) [49]. Santarnecci et al. showed a significant increase in cortical thickness in the right insula and the somatosensory cortex after an 8-weeks Mindfulness-Based Stress Reduction (MBSR) training program [47]. Pickut et al. reported increased grey matter density in the bilateral caudate, left cuneus, left thalamus, and left lingual gyrus in an 8-week mindfulness-based intervention randomised controlled trial (RCT) for Parkinson subjects who underwent mindfulness-based intervention [48]. In cross-sectional studies,

Author (published year)	Modality	Study design	Group type	Duration of MM training	Longitudinal?	Subjects	Results
Engen et al. 2017	Rs-fMRI (ALFF), cortical thickness	Cohort	17 long-term meditators (LTM) vs. 15 controls	(LTM has an average of 40k hours of meditation experience, control group has no prior experience)	no	healthy	Increased ALFF during meditation state vs resting state in long-term meditator. Increased thickness in the LTM cohort relative to meditation-native controls in fronto-insular cortices
Yang et al. 2019	Rs-fMRI (ALFF), cortical thickness	Cohort	No control group	40 days	Yes	healthy	Overlapping structural and functional effects in precuneus, where cortical thickness increased and low-frequency amplitudes (ALFF) decreased
Kral et al. 2019	Rs-fMRI (FC), diffusion tensor scans (DTI)	RCT	MBSR (N=48), active (N=47) or waitlist (N=45)	8 weeks	Yes (TP1,TP2,TP3)	healthy, meditation-naïve adults	Increased T2-T1 PCC-DLPFC resting connectivity for MBSR relative to control groups; increased PCC-DLPFC resting connectivity in MBSR participants was associated with increased microstructural connectivity of a white matter tract connecting these regions
Dodich et al. 2019	Rs-fMRI (FC), gray matter density	RCT	Training group vs. meditation-naïve group (control)	4-week Sahaja Yoga meditation	Yes	healthy	Compared with 30 control subjects, the participants to meditation training showed increased gray matter density and changes in the coherence of intrinsic brain activity in two adjacent regions of the right inferior frontal gyrus encompassing the anterior component of the executive control network

Figure 1.5: Mindfulness Meditation studies using resting-state fMRI and structural MRI

Kang et al. found increased cortical thickness in the superior frontal cortex, frontal medial prefrontal cortex, temporal areas for meditation subjects compared to the controls [33]. Finally, it has been demonstrated that the long-term practice of Sahaja Yoga Meditation leads to increased grey matter volume and regional enlargement in different cortical and subcortical brain areas which are correlated with compassion and interoceptive perception, sustained attention and self-control [50]. The recent work by Engen et al. investigated structural brain networks changes of long-term mental training effects on socio-affective skills [51]. These authors conducted both functional and structural analyses and found that ALFF increases in several prefrontal and insular areas during meditation relative to resting, and they also observed cortical changes. In figure 1.3, 1.4 and 1.5 the neuroimaging studies on Mindfulness Meditation using resting-state fMRI, structural MRI and both modalities are summarized.

## **1.6 Mindfulness Meditation Intervention for Depression**

### 1.6.1 Clinical Evidence

There is strong evidence that mindfulness meditation has therapeutic effects for example on emotion regulation [52–56]. As stated in Yang (2019), "Mindfulness meditation practice primarily leads to reductions in ruminative thinking, even after controlling for decrements in affective symptoms and dysfunctional beliefs [57]. In patients with affective disorders, mindfulness meditation intervention has been shown to improve anxiety and mood symptoms [54]. At a behavioural level, several studies have indicated that mindfulness-based therapy is a promising approach for treating anxiety and mood disorders [58–60]" [1]. Hilton et al. conducted systematic review on randomized controlled trials (RCTs) along with meta-analyses of mindfulness meditation as intervention for chronic pain, they found that the quality of life and depressive symptoms were improved significantly [61]. A recent study from Lopez-Maya E et al also reported improvement in depressive symptoms after mindfulness meditation training in an RCT [62]. Further, Black et al and colleagues also reported that the mindfulness meditation intervention is linked to improvement in sleep quality [63]. Saeed et al reported the benefits of exercise, yoga, and mindfulness meditation on depression and anxiety disorders, they found that mindfulness-based meditation (as monotherapy or an adjunctive therapy) has positive effects on depressive symptom, and its effects can last for six months or longer [64].

### 1.6.2 Clinical Rational

Depression has become the global awareness, according to the World Health Organization (WHO), there are around 350 million people with depression. Depression accounts for the largest share of the worlds burden of disease, which is measured by years lost to disability (YLD). Increasing evidence showed that meditation could be used to maintain daily mental healthy life or to treat depression. Numerous researchers have conducted cross-sectional

studies on mindfulness meditation, however, there are scant longitudinal studies which investigate the resting network plasticity changes in brains of meditation-naïve subjects, and it is normally performed by using either structural or functional imaging technique.

### 1.6.3 Mechanistic Evidence

The mechanistic evidence of mindfulness meditation as an alternative intervention method were fully introduced in [2]:

Recent findings suggest an altered resting state functional connectivity of the DMN of depressed patients compared to healthy participants [65]. Among these DMN regions, dorsal medial prefrontal cortex (dmPFC) was shown to be involved in self-inspection [66] and emotion regulation [67] and demonstrated increased activity in depression [68]. Thus, major depressive disorder (MDD) patients show more neural functional connectivity between the posterior cingulate cortex and the subgenual-cingulate cortex during rest periods compared to healthy individuals [69]. Several regions of anterior cingulate are of importance in depression-related disorders. Pregenual anterior cingulate cortex (pgACC) has been shown to be hypoactivated in MDD [70]. The dorsal anterior cingulate cortex (dACC) is associated with the involvement of cognitive control over attentional resources [71, 72], and it is strongly impaired in MDD. Van Tol et al. [73] showed that dACC and pgACC are also structurally affected in MDD, while pgACC was furthermore found to be molecularly affected by altered glutamate concentrations. In contrast to the dACC, the pgACC belongs to an affective subdivision of the ACC [71] and was shown to mediate the increased internal focus present in the ruminative thinking style of depressed patients. Furthermore, the pgACC is specifically impaired in highly anhedonic patients [74]. The neurobiological model of depression [75] states that impaired cognitive control, mediated by regions in the prefrontal cortex (PFC), cooccurs with hyperactivation of the amygdala, which facilitates encoding and retrieval of emotional stimuli via modulation of hippocampal activity. Activity in the medial prefrontal cortex (MPFC), which is associated with internal repre-

sentations of the self, is consequently increased as well. The suppressed regulatory influence of PFC regions facilitates an undesired recall of negative (mood-congruent) events. The DMN has been shown to support internally oriented and self-referential thoughts and MDD has been associated with both hyperconnectivity within the DMN and hyperconnectivity between frontoparietal control systems and regions of the default network [76]. Furthermore, MDD has been characterized by hypoconnectivity within the frontoparietal network, a set of regions involved in cognitive control of attention and emotion regulation, and hypoconnectivity between frontal systems and parietal regions of the dorsal attention network involved in attending to the external environment [76]. These networks modulate affective and cognitive processes disturbed in depression. In the cases described here, impairment refers to increase or decrease of an existing functional connection. Alterations reflect changes in operational properties of interregional connections and their local resting state activity. As much as MDD is characterized by hyperactivity in, for example, ventral and subcortical regions, this was discussed to be directly related to hypoactivity and resulting disinhibition from dorsal cortical regions [75]. Likewise, within-network connectivity can be altered in opposite direction compared to between-network connectivity (in terms of functional connectivity) as soon as a hub region is concerned, which connects both to its own functional module and towards regions outside its own functional subnetwork.

## **1.7 Specific Aim of the Thesis**

The specific aim of the current thesis was fully addressed in [1]:

The purpose of this study was to investigate structural and functional brain network changes (e.g. DMN) after 40 days of mindfulness meditation training in novices and set these in the context of potentially altered depression symptomatology and anxiety. This study aims to explore whether behavioural, structural and local functional brain changes are associated with short-term mindfulness meditation training.

### 1.7.1 Aims on Multi-modality

The aims of using multi-modality in the current thesis was introduced in [1]:

Longitudinal studies observing resting network plasticity effects in brains of novices who started to practice meditation are scarce and generally related to one dimension, such as structural or functional effects. In this thesis I aimed to discover the longitudinal brain changes by using both structural Magnetic Resonance Imaging (MRI) and functional Magnetic Resonance Imaging (fMRI).

### 1.7.2 Hypotheses

The hypotheses of the current thesis was introduced in [1]:

I hypothesised that the repeated activation of brain regions corresponding to the brain networks recruited during meditation training might induce congruent early structural and functional activity changes within relevant circuits. Based on prior findings, these were hypothesised to concern the default mode network (DMN). I further hypothesised if these brain changes were associated with potential behavioural changes in depression and anxiety scores.

## **CHAPTER 2**

### **GENERAL METHODS**

#### **2.1 Subjects**

Subject recruitment procedure is presented in this section is adopted from [2]:

28 university students (Spanish native speakers) were recruited by university advertisement to participate in the mindfulness meditation course. Sample demographic characteristics are detailed in Table 3.1. All study protocols were approved by the Institutional Review Board of the Universitat Jaume I of Castellon and informed consent was obtained from all subjects. Participants were screened for psychiatric or neurological conditions prior to enrollment in the meditation course. No previous meditation experience was reported by the subjects.

#### **2.2 Mindfulness Meditation Study Details**

Study design and the mindfulness training procedure are presented in this section are adopted from [2]:

##### 2.2.1 Study Design

In this longitudinal neuroimaging study each participant were scanned twice at the same MR scanner with the same setting (before and after meditation training). The study was designed that the experiment was performed at 3 different timepoints; namely, time point 1 (TP1), time point 2 (TP2) and time point 3 (TP3). Before the training of mindfulness meditation, subjects underwent a single resting state (RS) scan (TP1). Later on, at day 40 (TP2) and day 90 (TP3) subjects underwent two scans, a RS scan and a scan during which



they practiced meditation (meditation state, MS).

During the RS, subjects were instructed to close their eyes, to be in a normal relaxing condition without engaging in any specific task or mental activity, and not to fall into meditation. During meditation scan, subjects were instructed to close their eyes, openly monitor the surrounding environment by accepting all sensations rise and fall non-judgmentally, and specifically to be aware of the present moment as they were trained. At time point 2 (TP2) and time point 3 (TP3), RS scan was measured for 9 minutes followed by continuous MS lasting for 12 minutes. Long time acquisition for both conditions was set to obtain sufficient power for the functional connectivity analyses given the relatively small sample size [77].

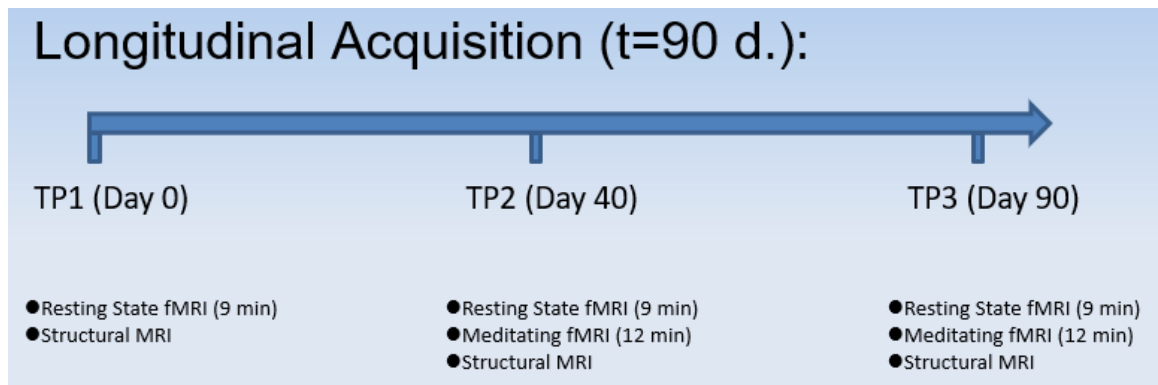


Figure 2.1: Study design- longitudinal MR imaging acquisition. At day 0 (TP1), I only acquired resting-state fMRI scans and structural MRI scans. While at day 40 (TP2) and day 90 (TP3), in addition to these two scans I acquired meditation scan, in which the subjects performed meditation while I ran the Echo-planar imaging (EPI) sequence

### 2.2.2 Mindfulness Meditation Training

The mindfulness training programmes consisted of 8 week courses, with daily practise at home in sessions of around 45 minutes [78]. The mindfulness-based stress reduction (MBSR) programme [3] as well as acceptance and commitment therapy [79] were used to design the meditation-mindfulness training programme based on self-observation training. The self-observation training programme consisted of eight 1.5 hour sessions over a period

of 8 weeks. The first hour of the sessions was devoted to simple physical and breathing exercises during which the participants were instructed to perform Vipassana meditation exercises, by focusing their attention on thoughts that came to their mind without dwelling on any of them.



Figure 2.2: 8-week mindfulness meditation training course (on site training + minimum 10 minutes daily home practice), which includes simple physical and breathing exercises and Vipassana meditation exercises

After the exercises, participants meditated in silence, continuing to observe their thoughts without censoring them. The time devoted to meditation without the physical exercises gradually increased over the course. The final half hour was used to talk about the experience and explain the characteristics of meditation and mindfulness in which videos and fables reflecting the most significant aspects of the meditation and self-observation experience were used. Participants were also encouraged to do the meditation exercises at home;

they were given a meditation diary in which to record their daily experiences, which was handed in to the course instructor. A quantification of the participants' amount of meditation practice at the end of the course is detailed in Table 3.1.

### **2.3 Self-report Measures**

I used behavioral measure reports to track the behavioral changes before and after the meditation training as published in [1]:

Total three self-assessment questionnaires were administered to participants both before and after the training period. I applied the Profile of Mood States (POMS) throughout the study in its abbreviated, Spanish version [80] of the original POMS [81]. It is a 44-item inventory, which measures current mood state by rating statements on a Likert scale (0 to 4). It consists of six subscales: anger, fatigue, tension, depression, vigor, and friendliness. To evaluate changes in depressive symptoms of our sample, I used the Center for Epidemiologic Studies Depression Scale (CES-D) which is a well-validated, 20-item inventory [82]. Subjects were asked to rate statements based on the previous week on a Likert scale (0-3) and scores range from 0 to 60, whereat higher scores indicate higher levels of depression. The State-Trait Anxiety Inventory [83] is a 40-item scale designed to measure the state and trait anxiety based on a Likert scale (1-4), which was also applied. Scores range from 20 to 80 whereat higher scores relate to higher levels of anxiety. To explore dimensions of potential effects on mindfulness, I further accessed the mindfulness measure Five Facet Mindfulness Questionnaire (FFMQ) before and after the meditation training [84]. Specifically, I assessed the facets of nonreactivity to inner experience, observation, acting with awareness, describing, non-judgment of experience. Participants responded on a 9-point Likert-type scale (1= never or rarely, 9 = almost always or always true) both before (TP1) and after (TP2) meditation training, with higher scores indicating higher self-reported mindfulness skills.

## 2.4 Data Details

The following section summarizing the data acquisition, MR imaging parameters and data preprocessing details as published in [2]:

### 2.4.1 Data Acquisition

In this longitudinal neuroimaging study participants were scanned twice. Before the training of mindfulness meditation, subjects underwent a single resting state (RS) scan (TP1). Later on, at day 40 (TP2), subjects underwent two scans, a RS scan and a scan during which they practiced meditation (MS). During the RS, subjects were instructed to close their eyes, be at the normal relaxing condition without engaging in any specific task or mental activity, and not fall into meditation. During meditation scan, subjects were instructed to close their eyes, openly monitor the surrounding environment by accepting all sensations rise and fall non-judgmentally, and specifically to be aware of the present moment as they were trained. At time point 2 (TP2), RS scan was measured for 9 minutes followed by continuous MS lasting for 12 minutes. Long time acquisition for both conditions was set to obtain sufficient power for the functional connectivity analyses given the relatively small sample size [77].

### 2.4.2 MR Sequence Parameters

Magnetic resonance measurements were performed on a 1.5 T Siemens AVANTO scanner (Siemens Erlangen, Germany). A structural image was acquired from each subject with a magnetization-prepared rapid gradient-echo (MP-RAGE) sequence (TR = 2200 ms, TE = 3.79 ms, flip angle (FA) = 15, 160 slices, matrix size = 256 x 256, field-of-view (FOV) = 256 mm x 256 mm, slice thickness = 1 mm). For both RS and MS, a standard EPI sequence was used (TR = 2300 ms, TE = 55 ms, FA = 90°, FOV = 224 mm x 224 mm, matrix size = 64 x 64, slice thickness = 4 mm,) with 25 axial slices for whole-brain coverage. Finally, an

extra gradient field mapping sequence (`gre_field_mapping`) was acquired followed by each EPI sequence (TR = 487 ms, TE1 = 8 ms, TE2 = 12.76 ms, FA = 65°, FOV = 224 mm x 224 mm, matrix size = 64 x 64, slice thickness = 4 mm) with 25 slices with the same coverage used in EPI sequence.

### 2.4.3 Data Preprocessing

B0 inhomogeneity correction was performed to reduce static field inhomogeneity using an EpiUnwarping tool based on FSL (<http://surfer.nmr.mgh.harvard.edu/fswiki/epidewarp.fsl>) [85]. Pre-processing was performed using Statistical Parametric Mapping (SPM8, <http://www.fil.ion.ucl.ac.uk/spm/>) and Data Processing Assistant for Resting-State fMRI (DPARSF v 2.3; [86]). Functional images were slice-time corrected. Motion correction was performed by using a least squares approach and a six-parameter (rigid body) linear transformation. Spatial normalization to MNI space was carried out by using unified segmentation of T1-weighted acquired images, and the extracted normalization parameters from segmentation were applied to normalize the functional volumes for each participant (voxels were re-sampled to 3-mm isotropic). Finally, functional volumes were smoothed by applying a 4 mm FWHM Gaussian kernel. Smoothed volumes were used for ICA and seed-based FC. ReHo analysis was performed on non-smoothed functional volumes and images were smoothed after the analysis, because smoothing prior to ReHo calculation would increase regional similarity [86]. I conducted additional preprocessing for seed-based FC and ReHo analyses using the DPARSF tool through the following steps: (i) removing a linear trend in the time series, (ii) temporally band-pass filtering (0.01-0.08 Hz) to reduce the effect of low-frequency drift and high-frequency noise [18, 87]. For the seed-based FC analysis, several sources of spurious variance were removed from the data through linear regression: six parameters from rigid body correction of head motion, white matter signal, cerebrospinal fluid signal, and the global mean signal [88]. For MS, the first and the last 40 volumes of the functional images were

discarded (total 313 volumes were acquired before removing the 80 volumes). The reason to remove the first 40 volumes was to allow the participants to get used to the scanning environment and ensure a reasonable establishment of the meditation state. The reason to remove the last 40 volumes was aim to avoid distraction effects at the end of the meditation, yielding a duration similar to the RS. The central 233 (8 min 33 sec) functional volumes of the times series were sufficient for estimation of Independent Components (ICs) [77].

## **2.5 Brain Function - Resting-state fMRI (rs-fMRI) Analysis**

In order to investigate the functional brain changes due to meditation training, the functional MRI data analysis of resting-state data were performed, namely the Functional Connectivity Analysis, Group Independent Component Analysis, and ReHo Analysis presented in the following section were published in [2]:

### 2.5.1 Functional Connectivity (FC) Analysis

#### *Seed-based Functional Connectivity*

I performed a hypothesis-driven seed-based FC analysis. Two independent seed ROIs placed in the pregenual anterior cingulate cortex (pgACC) and the dorsal anterior cingulate cortex (dACC) were chosen based on previous reports on their involvement in meditation and affective disorders such as depression [89]. To examine FC in the pgACC and the dACC in a whole brain voxel-wise analysis, these two seed regions were defined by the Montreal Neurological Institute (MNI) coordinates (x, y, z): 0, 41, 9 (pgACC) and 0,27,30 (dACC). Both ROIs had a radius of 10mm resulting in a volume of approximately 4ml, maximizing the gray matter contribution as described previously [90], as shown in Figure2.3. The averaged time course from each seed region was obtained for each subject at both timepoints and for both conditions (RS, MS) separately. An individual FC map for each seed was generated by calculating the voxelwise correlation coefficients in the whole

brain, which were then converted into z-maps by Fishers Z transformation to enhance normality. The z-maps of the dACC and pgACC of each individual were entered into second level paired t-test.

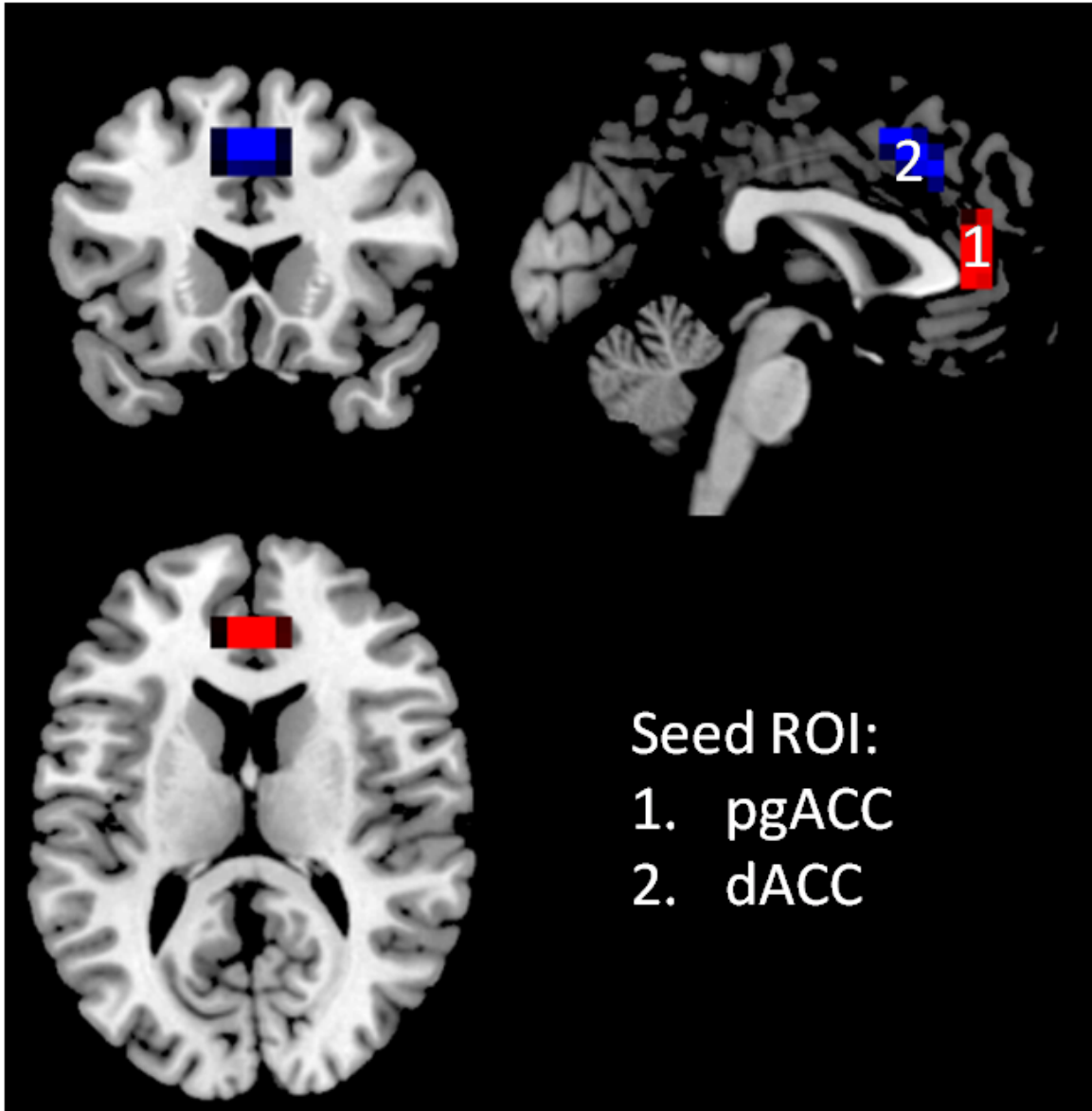


Figure 2.3: Seed ROIs used for RSFC analysis. ROI1: pregenual ACC (pgACC) as marked in red color. ROI2: dorsal ACC (dACC) as marked in blue color overlaid on the T1 anatomical MNI space [2]

### *Group Independent Component Analysis (Group ICA)*

In addition to the hypothesis-driven seed-based FC analysis, a data-driven approach - group independent component analysis was performed using GIFT (v 2.0e, <http://mialab.mrn.org/software/gift>)[91] to investigate: a) the training-related RSFC changes; and b) the FC difference between RS and MS. These analyses were performed based on FC analysis from spontaneous BOLD activity from the average fMRI time course of the entire brain. In the analysis of training-related RSFC changes over time, the longitudinal resting state data were grouped together when conducting group ICA following a previous report [92]. In the analysis of FC differences between RS and MS experimental conditions, a single ICA was performed at the group level for RS and MS conditions separately, in agreement with previous studies [93], [94]. The data of each condition was restricted to twenty-four independent components (ICs) using the MDL criteria and extracted by ICA decomposition using the Infomax algorithm [95]. To determine the reliability of the ICA algorithm, multiple runs of ICA were performed using ICASSO. Each IC consists of a spatial map and an associated timecourse. The ICs which resembled the DMN most were firstly spatially sorted by using the DMN template built-in in GIFT [91] and then further identified by visual inspection by two different raters for RS and MS separately. Subsequently, individual subject maps were back reconstructed to obtain single-subject results. Finally, the resulting individual IC maps were converted into voxel-wise z-score maps representing the degree to which each voxel belong to the overall ICA component map. Individual subject z-maps were entered into SPM random-effect analyses. The RSFC analysis involved a longitudinal analysis of changes in temporal correlations in connectivity fluctuations before and after training. To compare RS and MS conditions, one paired t-test was performed. In the IC decomposition, only DMN was extracted to be compared between timepoints and conditions. I computed the DMN from the average fMRI time course from the entire network as described before. Furthermore, in the analysis between RS and MS, the DMN comparison was not restricted to a mask of the conjunction between both condi-



tions, since it would involve the restriction of any other regions that may be identified as the DMN in the MS as different from the DMN in the RS, but to the addition of the masks for the DMN identified under RS and MS. Additionally, exploratory mask restricted analysis was performed, but not reported because its contribution was similar to the unrestricted comparison in the target regions of the DMN, although covering differences in other out regions.

### 2.5.2 ReHo Analysis

ReHo images of the whole-brain for both MS and RS were generated using DPARSF. The voxel-by-voxel Kendall's coefficient of concordance (KCC, [96]) of the time series of a given cluster of 27 neighbouring voxels was calculated [97]. To reduce the global effects of individual variability across participants, the ReHo of each voxel was scaled by the mean value of whole-brain ReHo for each participant. A paired t-test was performed to identify the effects of meditation on ReHo during resting-state activity between TP1 and TP2. A second paired t-test was performed to identify the differences in ReHo between the resting states (RS) and meditation state (MS) at TP2. The resulting t-value maps of each contrast of interest was displayed after applying a statistical height threshold of  $p < 0.001$  for each voxel and a corrected cluster threshold at  $p < 0.05$ , as determined by a Monte Carlo simulation (see AlphaSim in AFNI <http://afni.nimh.nih.gov/pub/dist/doc/manual/AlphaSim.pdf>).

### 2.5.3 ALFF Analysis

For the analysis of low-frequency amplitude changes, ALFF method were performed, as published in [1]:

B0 inhomogeneity correction was performed to reduce static field inhomogeneity using an FSL EpiUnwarping tool (<http://surfer.nmr.mgh.harvard.edu/fswiki/epidewarp.fsl>) [85]. The similar rs-fmri data preprocessing procedure was carried out as in our previous pub-

lication [2]. The first 10 images for each subject were discarded to allow for steady-state longitudinal magnetisation. The remaining images were then preprocessed by Statistical Parametric Mapping (SPM8, <http://www.fil.ion.ucl.ac.uk/spm/>) and Data Processing Assistant for the resting state fMRI (DPARSF Version 4.3 [98]). Functional images were slice-time corrected. Motion correction was performed by using a least squares approach and a six-parameter (rigid body) linear transformation. One subject was excluded according to the criterion that head motion was restricted to less than 2 mm of displacement or 2 degrees of rotation in any direction. The frame-wise displacement value (FD\_Power) showed no significant difference between the time points ( $t = 1.488$ ,  $p=0.162$ ; see Figure B.2 in Appendix).

Spatial normalisation to MNI space was carried out by using the unified segmentation of the T1-weighted acquired images. The extracted normalisation parameters from segmentation were applied to normalise the functional volumes for each participant (normalised images were then resampled to 3 mm isotropic voxels). Nuisance variables were regressed out (head motion parameters, white matter signal, cerebrospinal fluid signal). Scrubbing with regression strategy was used to reduce the motion effect from the subjects [99]. The linear trends of the BOLD signals were regressed. I calculated ALFF by using DPARSF v 4.3. The time series for each voxel was first band-pass filtered (0.01 - 0.1 Hz) and then fast Fourier transformed (FFT) to acquire a power spectrum in the frequency domain. The square root of the power spectrum was obtained and averaged across a frequency of 0.01 - 0.1 Hz at each voxel. The averaged square root was then known as the ALFF. Further, ALFF of each voxel for each participant was divided by the global mean ALFF for standardization [44]. Finally, the whole-brain-mean scaled ALFF maps were smoothed by applying a 6 mm full-width-at-half-maximum (FWHM) Gaussian kernel prior to the statistical analysis.

## 2.6 Brain Structure - Structural Magnetic Resonance Imaging

To study the brain structural changes due to meditation training, cortical thickness analysis as well as subcortical volume analysis were carried out and are presented in the following section as published in [1]:

### 2.6.1 Cortical Thickness

#### *Structural Data Pre-Processing Pipeline*

Cortical thickness was calculated using the FreeSurfer 5.3 (Massachusetts General Hospital, Boston, U.S., <http://surfer.nmr.mgh.harvard.edu>) version. A three-dimensional model of cortical surface reconstructions computed from T1 MPRAGE images was utilised in the FreeSurfer 5.3 package. Technical details of the processing pipeline were described in previous publications [31, 100–103]. In short, non-brain tissue removal, automated Talairach transformation of each subjects brain, volumetric structures segmentation [31, 103], cortical surface inflation to an average spherical surface, intensity normalisation, as well as automated topology correction were executed [104, 105]. The transition between grey/white matter and the pial surface were calculated by detecting the greatest shift in intensity by surface deformation. The quality of grey matter/white matter/ cerebrospinal fluid segmentation was visually examined in each subject, and the subjects with inaccurate segmentation were then excluded. Each hemisphere was then parcellated automatically into 74 distinct cortical areas, also the volume and thickness of these regions were calculated [106].

#### *Longitudinal Structural Data Processing- Cortical Thickness- Longitudinal Two-Stage Model*

Vertex-wise analyses of cortical thickness changes were performed with Freesurfer. Firstly, each subject's image data were smoothed by using a Gaussian kernel with an FWHM of 15 mm. To investigate changes in cortical thickness associated with mindfulness medita-

tion training, the longitudinal Two Stage Model <sup>1</sup> implemented in FreeSurfer was executed. The first stage reduces the temporal data within each subject to a single statistic (percent change). The second stage correlates it with a behavioural covariate (see Post-hoc Correlation Analysis). An inverse consistent registration was used to create an unbiased within-subject template and images [85, 98]. The reliability and statistical power are significantly increased by using the common information from the within-subject template to initialize the processing steps (skull stripping, Talairach transforms, atlas registration, spherical surface maps and parcellations) [99]. The quality assurance toolbox - QATool (<https://surfer.nmr.mgh.harvard.edu/fswiki/QATools>) in FreeSurfer was used to test the quality of the surface reconstruction and segmentation. In order to calculate the cortical thickness changes after mindfulness training, the percent change (pc1) was used to obtain a cortical measure. PC1 is the rate of change  $((\text{thickness2} - \text{thickness1}) / (\text{time2} - \text{time1}))$ , unit: mm/year) with respect to the thickness at the first time point:

$$pc1 = \frac{\frac{(\text{Thickness at } TP2 - \text{Thickness at } TP1)}{(TP2 - TP1)}}{\text{Thickness at } TP1} (\text{unit} : \text{mm/year/mm})$$

It describes the percentage thickening/thinning at a given cortical location.

### 2.6.2 Subcortical Volume

The subcortical volumes were also calculated using the automated segmentation algorithm, assignment of a neuroanatomical label to each voxel, and volumetric measurement procedures implemented in the FreeSurfer. I obtained eight bilateral subcortical volumes (lateral ventricle, thalamus, caudate, putamen, pallidum, hippocampus, bilateral amygdala, and nucleus accumbens).

---

<sup>1</sup><https://surfer.nmr.mgh.harvard.edu/fswiki/LongitudinalTwoStageModel>

## **2.7 Statistical Analysis**

In order to evaluate the evidence the data, several statistical testing were carried out. The following section demonstrating behavioural data analysis and structural data analysis as well as correlation analysis were published in [1]:

### 2.7.1 Behavioural Data Analysis

Changes of depression (CES-D) and Anxiety scores (STAI-state and STAI-trait) were assessed by paired-t-tests with significance accepted for a Bonferroni corrected  $p < 0.05$  for 3 tests, based on prior publications on antidepressant effects [82]. To further explore the dimensions of behavioural effects, mindfulness questionnaires (FFMQ) and Profiles of Mood States (POMS) questionnaires were assessed for relevant changes in the respective subscales without a prior hypothesis on an individual item and results are considered significant for an uncorrected  $p < 0.05$  on an exploratory level.

### 2.7.2 Seed-based FC Analysis

Described in section 2.5.1.

### 2.7.3 Group ICA

Described in section 2.5.1.

### 2.7.4 ALFF Analysis

I performed a voxel-wise ALFF analysis to assess the whole brain amplitude of low-frequency fluctuations changes in mindfulness meditation training. A paired t-test was performed to test the whole brain longitudinal ALFF differences (two-tailed). Multiple comparisons were corrected at FDR cluster level of  $p < 0.05$  with a conservative initial voxel height threshold of  $p < 0.001$ .

### 2.7.5 Cortical Thickness Analysis

One-sample t-tests were performed by using percent thickness change as point measure. To correct for multiple comparisons, I used a Monte-Carlo simulation (mc-z; synthesized, smoothed z-field) within FreeSurfer to correct for multiple comparisons, and the results were then smoothed by the residual and repeated for 10000 iterations, by using a threshold of  $p < 0.05$  (two-tailed).

### 2.7.6 Subcortical Volume Analysis

The statistical analyses of subcortical volume changes were conducted using SPSS version 19 (IBM SPSS Statistics for Windows, Version 19.0. Armonk, NY: IBM Corp., <http://www.spss.com>). Demographic and clinical data were analyzed using paired samples t-tests (2-tailed). Data were normally distributed, as indicated by the Kolmogorov-Smirnov test. Paired t-tests were also applied to analyze subcortical volume differences for each ROI over time. Differences in subcortical brain volume between TP1 and TP2 were represented as time effects. For ease of comparison with future results of other studies, I reported the original uncorrected p-values for subcortical volume and whether they survived the FDR threshold.

### 2.7.7 Post-hoc Correlation Analysis

Regression models (one-sample t-tests) included percent thickness change (PC1) as an independent factor and above behavioural scores changes as dependent factors. Age and gender were included as nuisance covariates in all general linear model (GLM) analyses. Respective multiple comparisons correction was carried out in order to correct the type I error. A post-hoc Pearson correlation analysis was also calculated to investigate the relationship between the ALFF values and behavioural scores. Given that these analyses were exploratory in nature, a statistical significance level of  $p < 0.05$  was used. The analysis was set out on only those items from the questionnaires that revealed a significant main effect

of the intervention. Based on our behavioural results in this study, cortical thickness and ALFF changes were correlated with the significant changes in behavioural scores from the questionnaires CES-D and STAI-trait.

## CHAPTER 3

### RESULTS

#### 3.1 Subject Demographic

Total 28 subjects were attended for experiment, half (n=14) went to TP1 and TP2, the other half (n=14) went to TP1 and TP3. However, due to lacking of complete mindfulness meditation training (missing practice of meditation course as well as missing the documentation of home practice), 14 subjects which went to TP1 and TP3 were discarded from the final analysis. At the final stage, only 14 subjects which went to TP1 and TP2 were included for the final analysis. Specifically, for functional imaging data, one subject was excluded due to extensive head movement, finally total 13 subjects were included for functional analysis and results. For structural data, total 14 subjects were included for the analysis and results. The complete subject demographic and exploratory behavioral questionnaires were listed in Table3.1. In Table3.1, 14 subjects were listed, for the correlation analysis of functional data, only 13 subjects were included.

Table 3.1: Subject demographic and exploratory behavioural measures. Group mean and standard deviation are listed [1].

	<b>TP1</b> (mean $\pm$ standard deviation)	<b>TP2</b> (mean $\pm$ standard deviation)
Number of participants	14	14
Age (years)	24.53 ( $\pm$ 5.90)	24.64 ( $\pm$ 5.90)
The ratio of males and females	4/10	4/10
Minutes of meditation practice per day	0	10.84 ( $\pm$ 8.41)
Total number of meditation days until scanning	0	39.23( $\pm$ 3.63)
Total number of minutes of meditation practice until scanning	0	423.41( $\pm$ 30.56)



## 3.2 Results of Behavioral Self-report Measures

The results of behavioral measures both before and after the mindfulness training are presented in the following section [1]:

### 3.2.1 Behavioral Self-report Measures

The primary behavioural outcome for the subjects is summarized in Table 3.2. The total scores of CES-D showed a significant reduction, controlled for multiple comparisons, of depression scores after meditation training ( $t(13) = 4.402$ ;  $p < 0.001$ ). STAI measures showed a significant reduction in trait anxiety ( $t(13) = 2.73$ ;  $p < 0.01$ ), but not in state anxiety scores after meditation training. The demographic and exploratory behavioural information for the subjects is summarized in Table 3.3. No significant change was observed of the POMS sub-scores. The FFMQ factor - nonreactivity to inner experience showed a significant increase after meditation training ( $t(13)=6.2$ ;  $p < 0.001$ , uncorrected for multiple comparisons).

Table 3.2: Primary behavioural outcome<sup>1</sup>(n=14) [1]

	<b>TP1</b> (mean $\pm$ standard deviation)	<b>TP2</b> (mean $\pm$ standard deviation)
CES-D	15.57 ( $\pm 9.49$ )	8.71 ( $\pm 6.06$ )***
STAI-state	17.93 ( $\pm 4.58$ )	13.57 ( $\pm 10.23$ )
STAI-trait	22.50 ( $\pm 9.39$ )	16.36 ( $\pm 9.37$ )**

## 3.3 Brain Function - Functional Brain Imaging Results

The results of both cross-sectional and longitudinal analysis of functional brain imaging data are presented in the following section as in [2]:

<sup>1</sup>Mean values (standard deviation) for each variable are shown before (TP1) and after (TP2) mindfulness training. CES-D, Center for Epidemiologic Studies Depression Scale; STAI, State-Trait Anxiety Inventory; POMS, Profile of Mood States; FFMQ, Five Facet Mindfulness Questionnaire. Significant group differences: \*\*\*: significant at  $p < 0.001$ , \*\*: significant at  $p < 0.01$ . (+): positive mood state factor, (-): negative mood state factor.

Table 3.3: Exploratory behavioural measures (n=14) [1]

	TP1 (mean $\pm$ standard deviation)	TP2 (mean $\pm$ standard deviation)
POMS, Anger (-)	2.64 ( $\pm$ 3.71)	3.07 ( $\pm$ 5.90)
POMS, Fatigue (-)	4.57 ( $\pm$ 2.77)	3.43 ( $\pm$ 4.50)
POMS, Vigour (+)	11.85 ( $\pm$ 5.11)	12.50 ( $\pm$ 5.19)
POMS, Friendliness (+)	18.28 ( $\pm$ 3.72)	19.14 ( $\pm$ 4.27)
POMS, Tension (-)	7.64 ( $\pm$ 3.49)	5.07 ( $\pm$ 5.12)
POMS, Depression (-)	3.85 ( $\pm$ 3.79)	4.21 ( $\pm$ 7.82)
FFMQ, non-reactivity to inner experience	4.55 ( $\pm$ 0.83)	6.10 ( $\pm$ 1.19)***
FFMQ, observing	5.94 ( $\pm$ 1.42)	6.48 ( $\pm$ 1.68)
FFMQ, acting with awareness	4.12 ( $\pm$ 1.38)	3.99 ( $\pm$ 0.94)
FFMQ, describing	4.74 ( $\pm$ 0.48)	4.93 ( $\pm$ 1.41)
FFMQ, non-judging of experience	4.56 ( $\pm$ 1.09)	4.92 ( $\pm$ 0.86)

### 3.3.1 Seed-based FC

#### *Comparison of FC differences between RS and MS*

When I compared the functional imaging contrast between resting and meditation states (RS>MS), I observed that the pgACC showed a reduced connectivity with the bilateral inferior parietal gyri, but an increased connectivity with the MPFC, the left superior temporal gyrus (STG), and the right TPJ during MS as shown in Figure 3.1 and Table 3.4 ( $p < 0.05$ , FWE-corrected). Further, one can see that the dACC showed a decreased FC with the left anterior insula (AI) during MS ( $p < 0.05$ , FWE-corrected), see Figure 3.2 and Table 3.4. The voxel-wise significance level was set at  $p < 0.001$  with a spatial extent threshold of 16 contiguous voxels, yielding a whole-brain threshold of  $p < 0.05$  corrected for multiple comparisons using AlphaSim algorithm implemented in AFNI (data dimension: 61 x 73 x 61 voxels, Gaussian filter widths:  $FWHM_x = 6.66$ ,  $FWHM_y = 6.88$ ,  $FWHM_z = 6.79$ ).

#### *Longitudinal Analysis of RSFC Changes due to Meditation*

I also investigated the longitudinal effect of meditation practice (TP1>TP2) on RSFC separately for the seed of pgACC and dACC by contrasting their functional imaging contrast

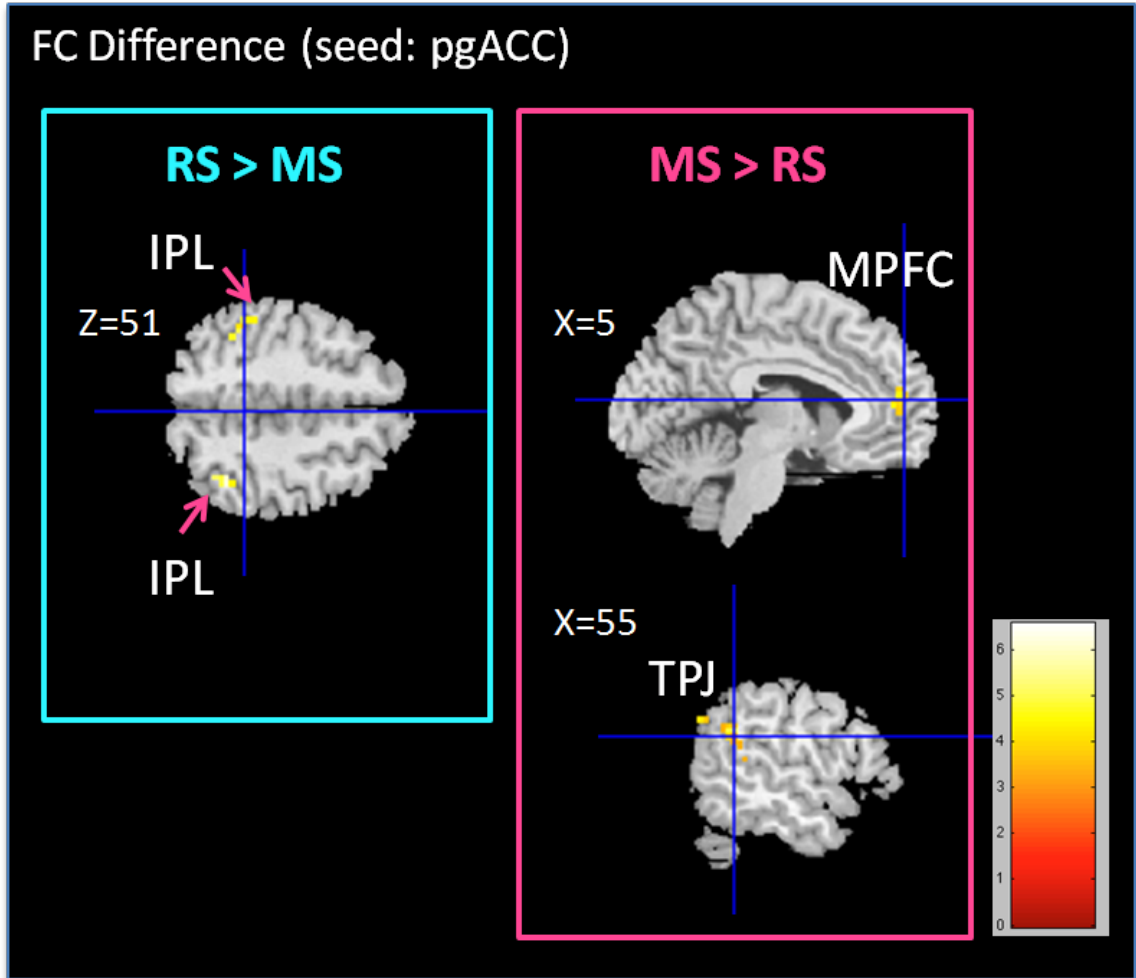


Figure 3.1: Paired comparison of seed-based FC maps (seed = pgACC) between rest and meditation at TP2 ( $p < 0.05$ , FWE-corrected). Bar plot represents the t-values. White labels indicate the coordinate of each slice in the MNI frame of reference (x, z). [2]

(TP1 vs. TP2). When using pgACC as an seed ROI in analysis, a decreased connectivity to the left PCC/precuneus, the left dorsal medial prefrontal cortex (dmPFC), the right superior temporal gyrus (STG), the left middle occipital gyrus, and left inferior temporal gyrus was observed, while connectivity to the right inferior temporal gyrus, the right inferior frontal gyrus (IFG), and the right TPJ/IPL increased after meditation training ( $p < 0.05$ , FWE-corrected, see Figure 3.3 and Table 3.5). While when using dACC as the seed ROI for analysis, meditation training entailed a reduction of RSFC to calcarine sulcus and the cuneus, but an increased RSFC towards cerebellum, the right inferior parietal lobe (IPL),

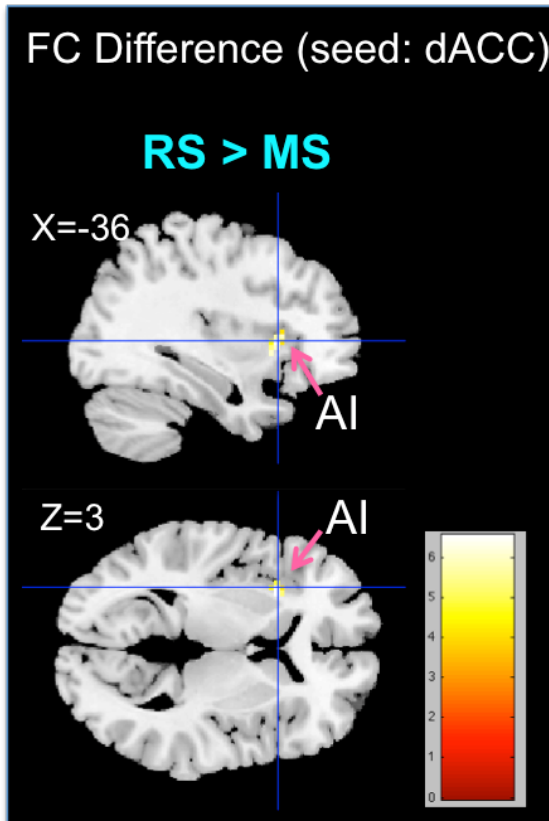


Figure 3.2: Paired comparison of seed-based FC maps (seed = dACC) between rest and meditation at TP2. FC decreases between dorsal ACC and left AI during meditation as compared to rest ( $p < 0.05$ , FWE-corrected). Bar plot represents the t-values. White labels indicate the coordinate of each slice in the MNI frame of reference ( $x, z$ ) [2].

and the posterior cingulate cortex (PCC) ( $p < 0.05$ , FWE-corrected see Figure 3.4 and Table 3.5). The voxel-wise significance level was set at  $p < 0.001$  with a spatial extent threshold of 16 contiguous voxels, yielding a whole-brain threshold of  $p < 0.05$  corrected for multiple comparisons using AlphaSim algorithm implemented in AFNI (data dimension:  $61 \times 73 \times 61$  voxels, Gaussian filter widths:  $\text{FWHM}_x = 6.66$ ,  $\text{FWHM}_y = 6.88$ ,  $\text{FWHM}_z = 6.79$ ).

### 3.3.2 Group ICA

#### *Comparison of the DMN independent component between RS and MS*

I want to ensure that our DMN comparison between these two conditions was performed in the same low-frequency band, power density spectra were obtained. The spectra results revealed that both DMNs were derived from the same very low frequency band ( $<0.04$  Hz). This insured that the comparison between RS and MS were performed in the same expected very low frequency domain [94], see Figure 3.5. At TP2, I found that the ICA results revealed reduced activation during meditation in dACC, sgACC, bilateral insula, superior frontal gyrus, and inferior frontal gyrus (IFG) when compared to rest ( $p < 0.05$ , FWE-corrected). The precuneus and the left temporo-parietal junction (TPJ) showed an increased internal consistency in the ICs during MS, see Figure 3.6 and Table 3.4. The voxel-wise significance level was set at  $p < 0.001$  with a spatial extent threshold of 16 contiguous voxels, yielding a whole-brain threshold of  $p < 0.05$  corrected for multiple comparisons using AlphaSim algorithm implemented in AFNI (data dimension:  $61 \times 73 \times 61$  voxels, Gaussian filter widths:  $\text{FWHM}_x = 7.39$ ,  $\text{FWHM}_y = 8.18$ ,  $\text{FWHM}_z = 8.19$ ).

#### *Longitudinal Analysis of RS Changes in the DMN Independent Component due to Meditation Training*

The paired t-test at a threshold of  $p < 0.05$ , FWE-corrected did not reveal longitudinal changes within the DMN independent components. The voxel-wise significance level was set at  $p < 0.001$  with a spatial extent threshold of 23 contiguous voxels, yielding a whole-brain threshold of  $p < 0.05$  corrected for multiple comparisons using AlphaSim algorithm implemented in AFNI (data dimension:  $61 \times 73 \times 61$  voxels, Gaussian filter widths:  $\text{FWHM}_x = 7.84$ ,  $\text{FWHM}_y = 8.68$ ,  $\text{FWHM}_z = 8.53$ ).

### 3.3.3 ReHo

#### *ReHo Comparison between MS and RS*

The comparison of MS and RS (MS>RS) showed an increased ReHo in dACC, left striatum (putamen), MPFC, and TPJ (supramarginal gyrus), FWE-corrected at  $p < 0.05$ , see Figure 3.7 and Table 3.4. The voxel-wise significance level was set at  $p < 0.001$  with a spatial extent threshold of 63 contiguous voxels, yielding a whole-brain threshold of  $p < 0.05$  corrected for multiple comparisons using AlphaSim algorithm implemented in AFNI (data dimension: 61 x 73 x 61 voxels, Gaussian filter widths: FWHM<sub>x</sub> = 13.25, FWHM<sub>y</sub> = 13.98, FWHM<sub>z</sub> = 12.13).

#### *Longitudinal Analysis of ReHo Changes*

Longitudinal effects of meditation on the ReHo of RS activity were tested between timepoints using a paired t-test. However, no significant differences between timepoints were found. The voxel-wise significance level for this analysis was set at  $p < 0.001$  with a spatial extent threshold of 70 contiguous voxels, yielding a whole-brain threshold of  $p < 0.05$  corrected for multiple comparisons using AlphaSim algorithm implemented in AFNI (data dimension: 61 x 73 x 61 voxels, Gaussian filter widths: FWHM<sub>x</sub> = 14.28, FWHM<sub>y</sub> = 14.53, FWHM<sub>z</sub> = 12.48).

### 3.3.4 ALFF

The results of low-frequency amplitude analysis and post-hoc correlation analysis are presented in the following section as published in [1]:

#### *Whole brain ALFF analysis result: ALFF changes after mindfulness meditation*

For the functional resting state fluctuations, I found ALFF decreased after meditation training also in left PCC/precuneus and, in addition to the structural findings, also in bilateral

IPL ( $p < 0.05$ , FDR-corrected, Figure 3.8).

### *Post-hoc Correlation Analysis Results*

I had also obtained the correlations between whole brain percentage cortical thickness changes and ALFF with significantly changing behavioural scores (CES-D, STAI-trait). Interestingly, on a whole brain level, changes in STAI trait scores were negatively correlated with percentage thickness changes in the left inferior temporal gyrus (Monte Carlo corrected,  $p < 0.05$ , Figure 3.10). For ALFF, there was no whole-brain corrected correlation of meditation-induced changes and changes in behavioural scores. Given the regional effects on PCC/precuneus, I extracted the delta mean ALFF values at left PCC/precuneus and correlated these with the delta CES-D and delta STAI-trait scores, respectively. I observed a negative correlation with delta CES-D,  $p = 0.024$ ,  $r = 0.619$  (Figure 3.9). Likewise, there were no significant correlations with these variables at baseline ALFF. When extracting cortical thickness in precuneus, there was no correlation with either score.

## **3.4 Brain Structure - Structural Brain Imaging Results**

The results of longitudinal structural brain analysis (cortical thickness) were carried out to investigate the impact of meditation training on brain structure as in [1]:

### 3.4.1 Cortical Thickness

*Structural whole cortex analysis: Cortical Thickness changes following mindfulness meditation*

Regional cortical thickness increased significantly (PC1) in left precuneus (MNI coordinates at peak vertex: [-12.7, -72.9, 40.7]; cluster wise  $p = 0.0003$ ) and left superior parietal lobule (peak vertex at [-8.8, -89.2, 21.4]; cluster-wise  $p = 0.01641$ ), corrected for multiple comparisons using Monte Carlo Simulation, (Figure 3.11).

### 3.4.2 Subcortical Volume

#### *Subcortical Volume Changes following mindfulness meditation*

Significant regional volume increased in right putamen ( $t = 2.391$ ,  $df = 13$ ,  $p = 0.033$ , uncorrected). In the subcortical volume analysis, I report uncorrected p-values with a significance threshold determined by Bonferroni correction for testing 16 regions of interest ( $p = 0.05/16 = 0.003$ ) as shown in Table 3.6 and Figure 3.12.



Analysis	Rest > meditation				Meditation > rest					
	Region	Side	K	MNI coordinates	z-score	Region	Side	K	MNI coordinates	z-score
ICA	dACC	R	202	9 21 36	5.70	Precuneus	R	178	3 -66 27	4.94
	sgACC	R	349	9 27 0	5.60	TPJ/IPL	L	157	-51 -57 27	4.31
	AI	L	336	-39 9 0	5.02					
	AI	R	37	45 18 0	4.34					
	IFG/BA9	R	21	60 18 27	4.26					
Seed-based FC (ROI: pgACC)	IPL	L	42	-45 -39 36	4.31	TPJ	R	58	57 -66 36	4.51
	IPL	R	45	39 -51 51	4.17	MPFC	R	36	9 51 9	4.49
						STG	L	23	-42 -60 18	3.86
						n.s.				
(ROI: dACC)	AI	L	20	-36 18 3	4.2					
ReHo										
	n.s.					dACC	R	125	0 36 15	5.32
						MPFC	R	125	6 48 12	4.24
						Putamen	L	77	-21 6 3	4.40

Notes: AI, anterior insula; dACC, dorsal anterior cingulate cortex; IPL, inferior parietal lobe; K, cluster size; MPFC, medial prefrontal cortex; pgACC, pregenual anterior cingulate cortex; sgACC, subgenual anterior cingulate cortex; STG, superior temporal gyrus; TPJ, temporoparietal junction; and BA: brodmann area.

<sup>a</sup>Family-wise error.

<sup>b</sup>A combined threshold of  $p < 0.001$  and a minimum cluster size determined by AlphaSim<sup>c</sup> algorithm in AFNI, resulting in FWE-corrected threshold of  $p < 0.05$ . An estimate of the spatial correlation across voxels was modeled using the program 3dFWHM<sup>d</sup> in AFNI.

<sup>c</sup>AlphaSim: <http://afni.nimh.nih.gov/pub/dist/doc/manual/AlphaSim.pdf>.

<sup>d</sup>3dFWHM: [http://afni.nimh.nih.gov/pub/dist/doc/program\\_help/3dFWHM.html](http://afni.nimh.nih.gov/pub/dist/doc/program_help/3dFWHM.html).

Table 3.4: Regions showing functional differences between conditions (rest versus meditation) [2]

Analysis	TP1 > TP2				TP2 > TP1					
	Region	Side	K	MNI coordinates	z-score	Region	Side	K	MNI coordinates	z-score
ICA				n.s. ( $p < 0.001$ , FWE <sup>a</sup> -corrected cluster threshold at $p < 0.05$ ) <sup>b</sup>						
Seed-based FC				( $p < 0.001$ , FWE-corrected cluster threshold at $p < 0.05$ ) <sup>b</sup>						
(ROI: pgACC)	PCC/precuneus	L	58	-12 -51 15	4.71	ITG	R	16	54 -63 -18	4.23
	dmPFC	L	49	-12 45 54	4.35	IFG	R	17	39 24 6	3.84
	STG	R	53	54 -63 15	4.34	IPL/TPJ	R	18	33 -60 42	3.76
	MOG	L	22	-24 -102 6	4.19					
	ITG	L	21	-57 0 -24	4.01					
(ROI: dACC)	Calcarine/cuneus	L	18	-9 -84 21	4.37	Cerebellum	L	22	-30 -54 -30	4.56
	BA19	L	26	-27 -90 21	4.01	IPL	R	16	36 -60 45	4.20
						PCC	R	19	3 -30 30	4.13
ReHo				n.s. ( $p < 0.001$ , FWE-corrected cluster threshold at $p < 0.05$ ) <sup>b</sup>						

Note: dmPFC, dorsal medial prefrontal cortex; IFG, inferior frontal gyrus; IPL, inferior parietal lobe; ITG, inferior temporal gyrus; K, cluster size; PCC, post cingulate cortex; STG, superior temporal gyrus; MOG, middle occipital gyrus; and BA: brodmann area.

<sup>a</sup>Family-wise error.

<sup>b</sup>A combined threshold of  $p < 0.001$  and a minimum cluster size determined by AlphaSim<sup>c</sup> algorithm in AFNI, resulting in corrected threshold of  $p < 0.05$ .

An estimate of the spatial correlation across voxels was modeled using the program 3dFWHM<sup>d</sup> in AFNI.

<sup>c</sup>AlphaSim: <http://afni.nimh.nih.gov/pub/dist/doc/manual/AlphaSim.pdf>.

<sup>d</sup>3dFWHM: [http://afni.nimh.nih.gov/pub/dist/doc/program\\_help/3dFWHM.html](http://afni.nimh.nih.gov/pub/dist/doc/program_help/3dFWHM.html).

Table 3.5: Regions showing RSFC differences between time points [2]

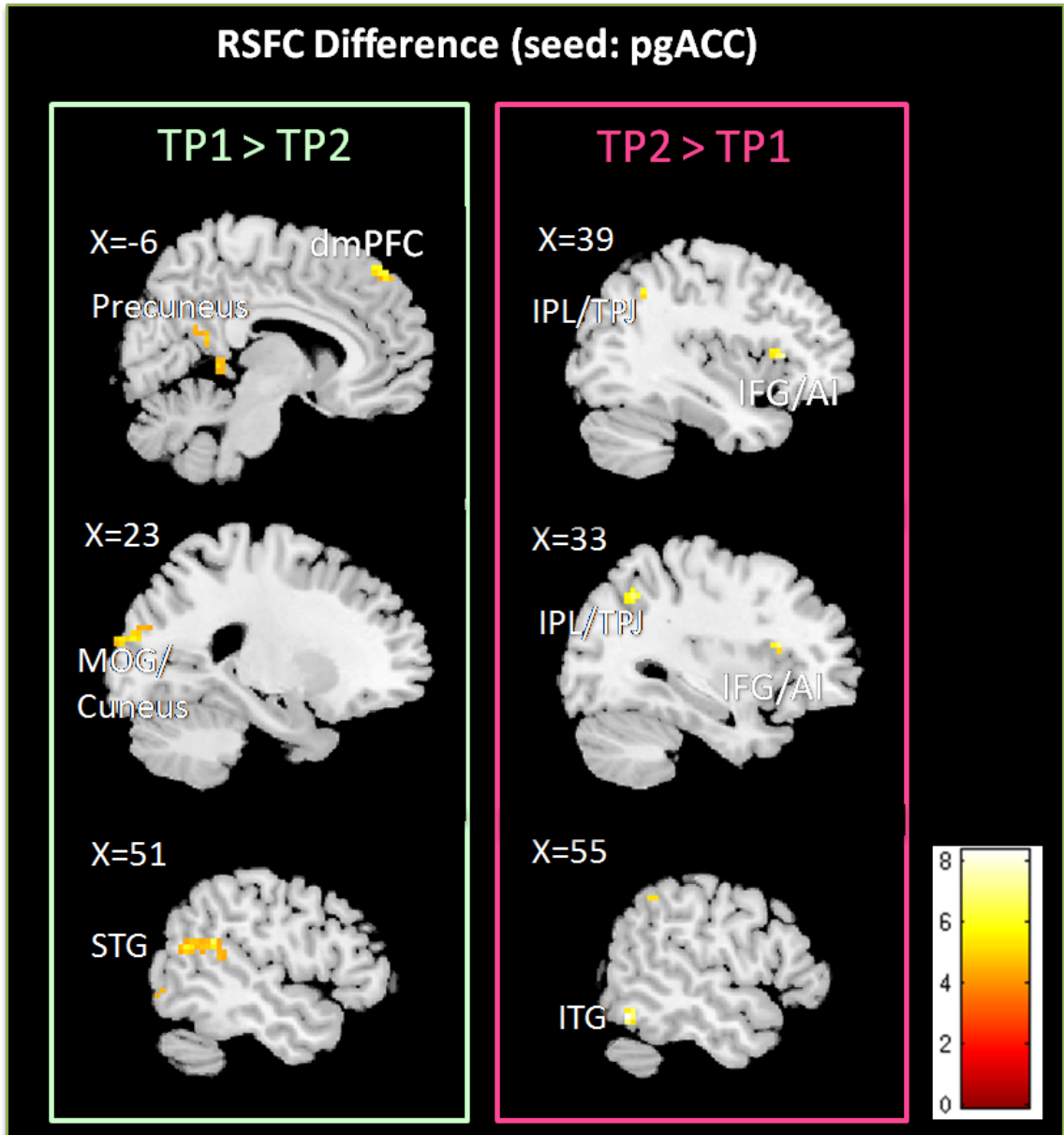


Figure 3.3: Longitudinal seed-based RSFC results (seed = pgACC). ( $p < 0.05$ , FWE-corrected). Bar plot represents the t-values. White labels indicate the coordinate of each slice in the MNI frame of reference (x, z) [2]

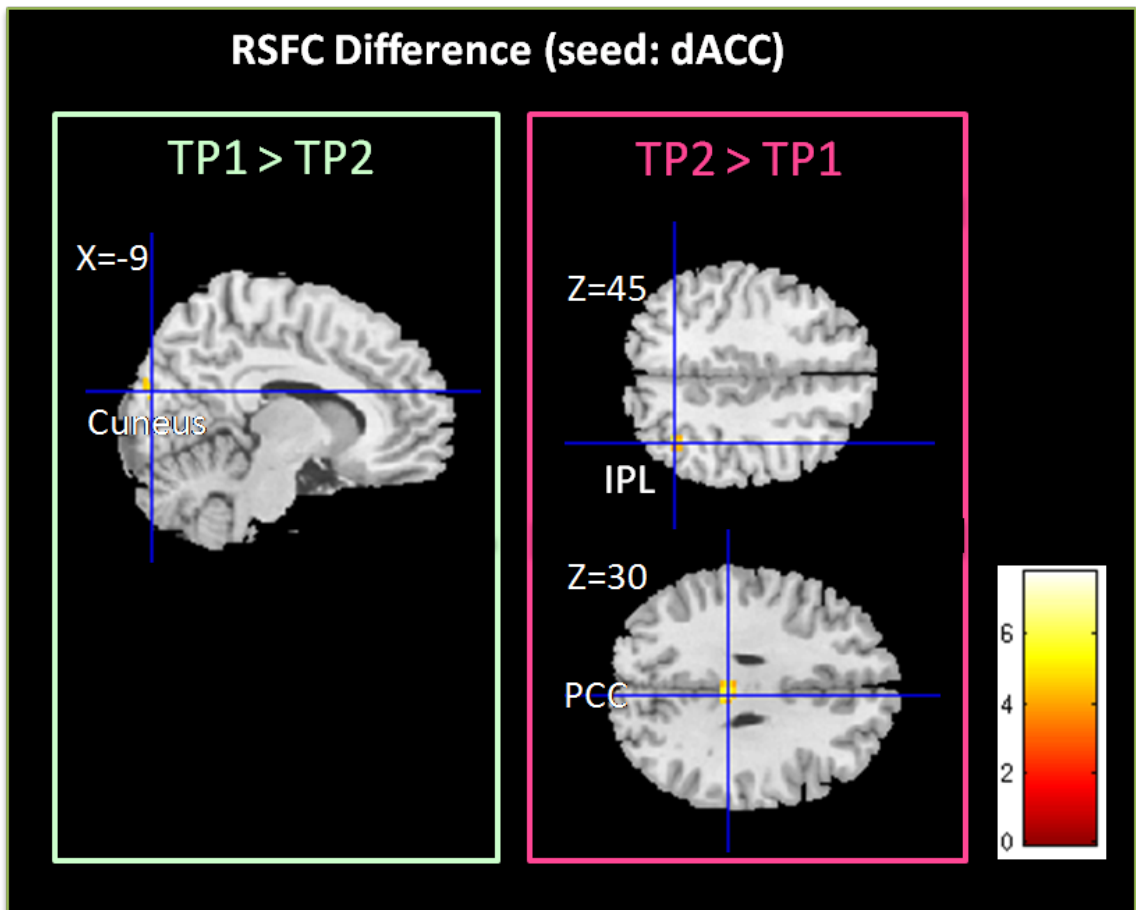


Figure 3.4: Longitudinal seed-based RSFC results (seed = dACC). ( $p < 0.05$ , FWE-corrected). Bar plot represents the t-values. White labels indicate the coordinate of each slice in the MNI frame of reference (x, z). [2]

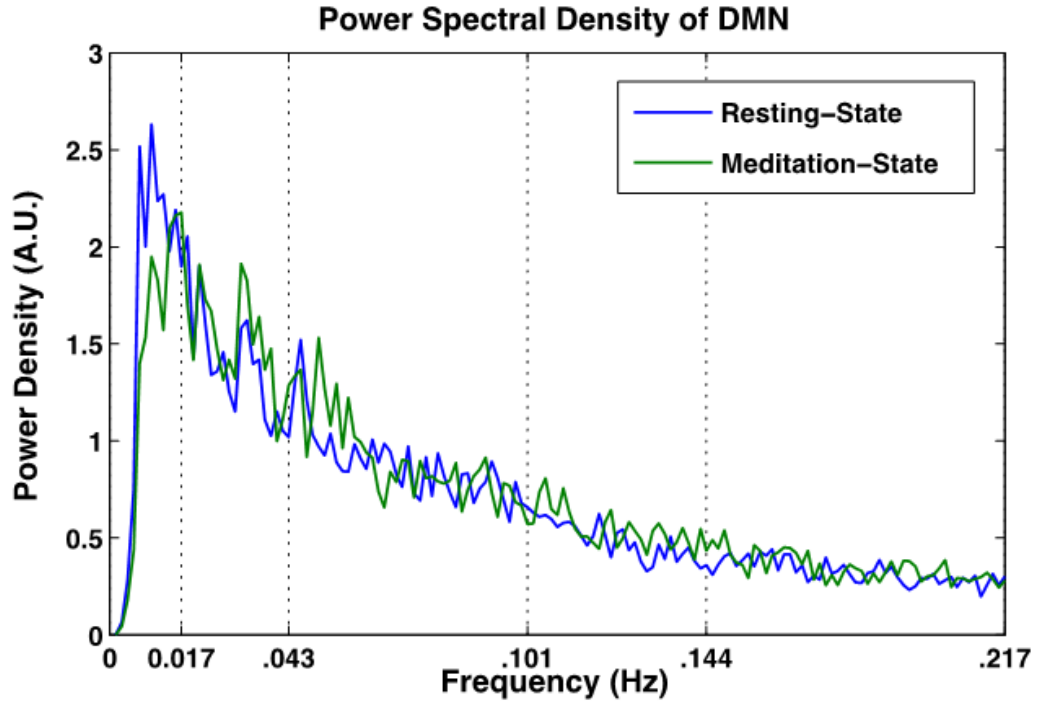


Figure 3.5: Mean power spectral density of the Default Mode Network (DMN) component. The peak power density was observed below 0.04 Hz for both conditions (Resting-State and Meditation-State). A.U. stands for arbitrary unit. [2]

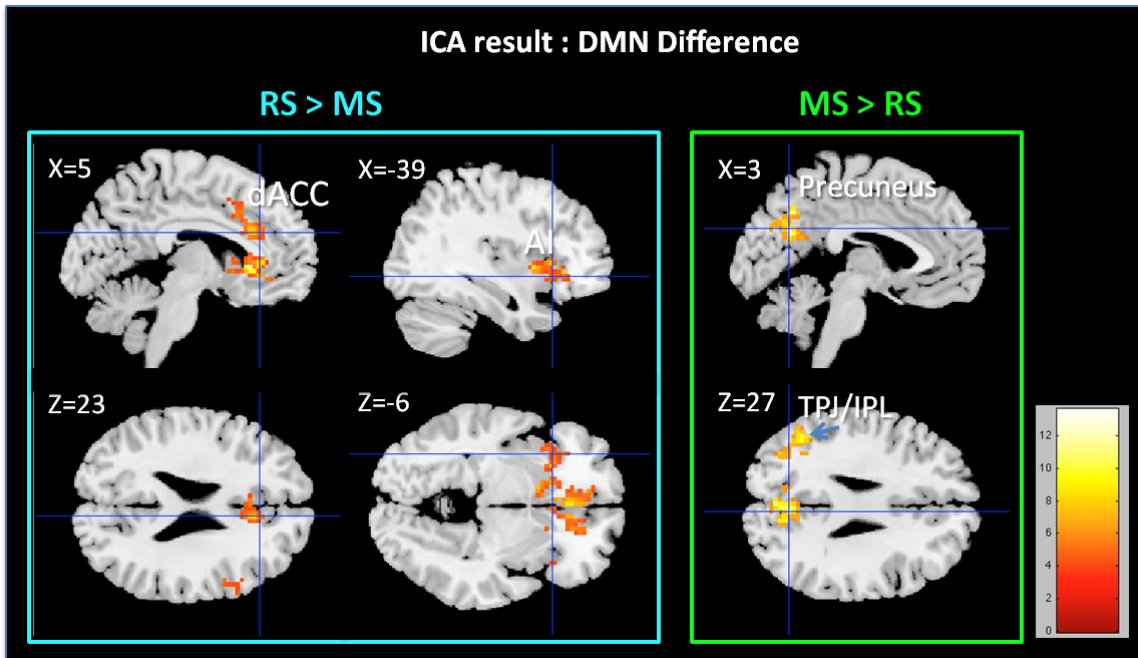


Figure 3.6: ICA results. DMN differences at TP2 for RS >MS and MS >RS ( $p < 0.05$ , FWE-corrected). Bar plot represents the t-values. White labels indicate the coordinate of each slice in the MNI frame of reference (x, z). [2]

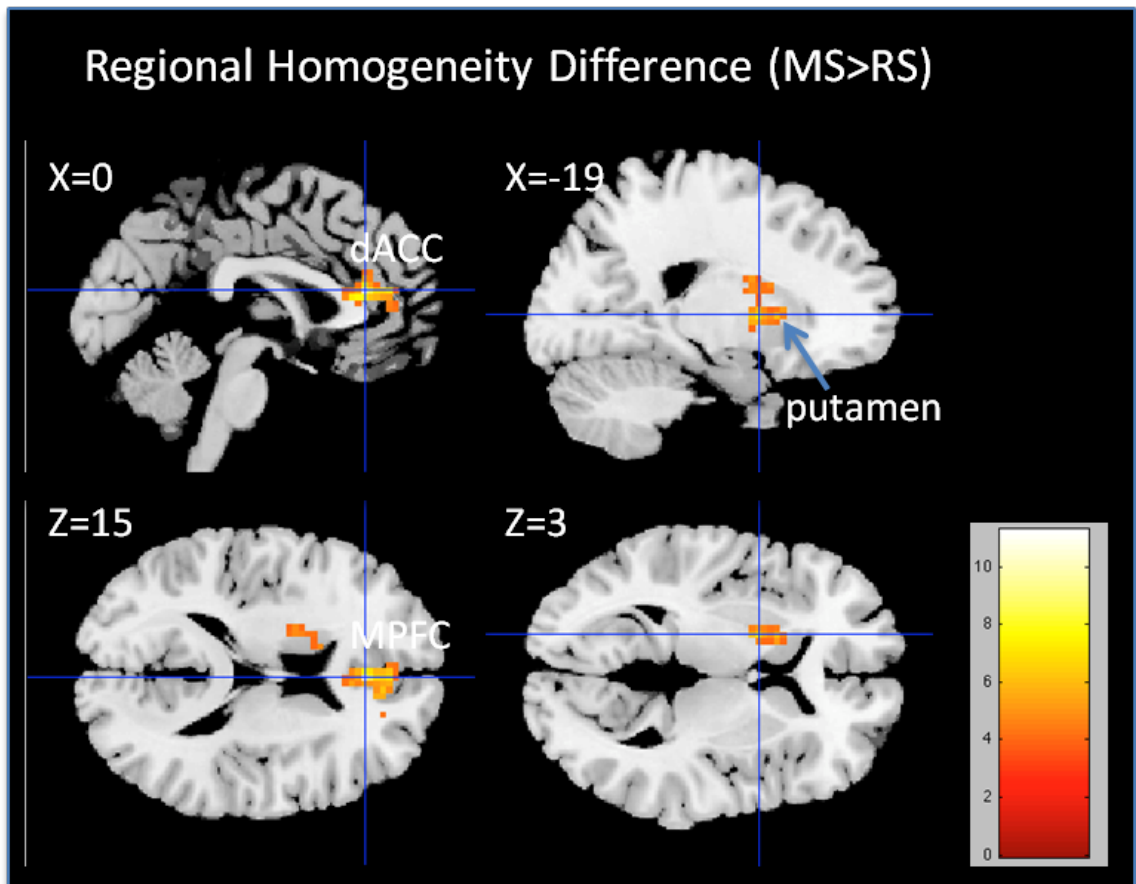


Figure 3.7: Regional homogeneity difference between MS and RS ( $p < 0.05$ , FWE-corrected). Bar plot represents the t-values. White labels indicate the coordinate of each slice in the MNI frame of reference (x, z). [2]

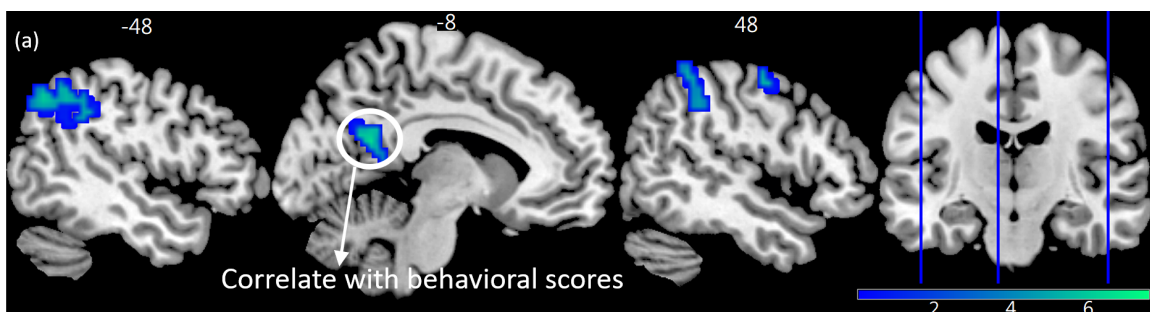


Figure 3.8: Longitudinal ALFF decreases after mindfulness meditation training (TP1 > TP2): Left IPL (Left angular gyrus), left PCC/precuneus and right IPL (right supra-marginal) were found (FDR corrected,  $p < 0.05$ ). Colorbar shows the t-values. [1]

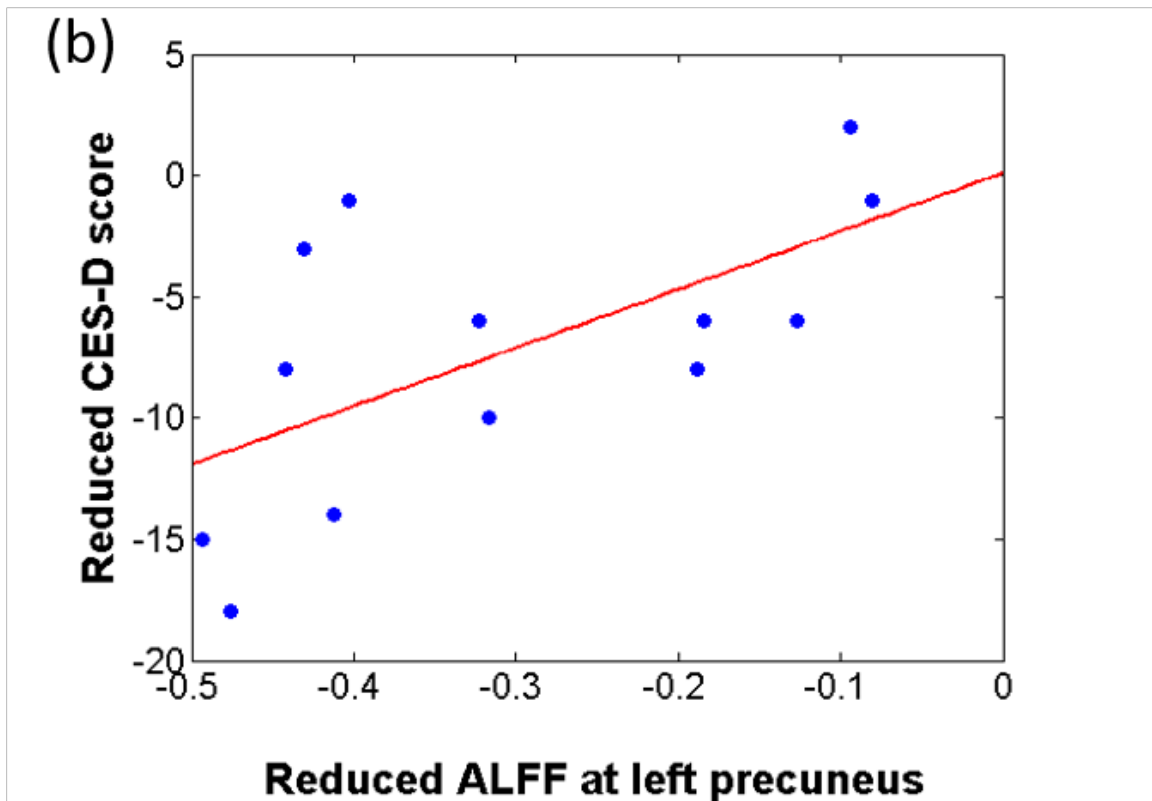


Figure 3.9: Post-hoc correlation of mean ALFF at left PCC/precuneus with CES-D. Decreased ALFF at left PCC/precuneus was found positively correlated with the reduction of depression score (CES-D),  $p=0.024$ ,  $r=0.619$ . [1]

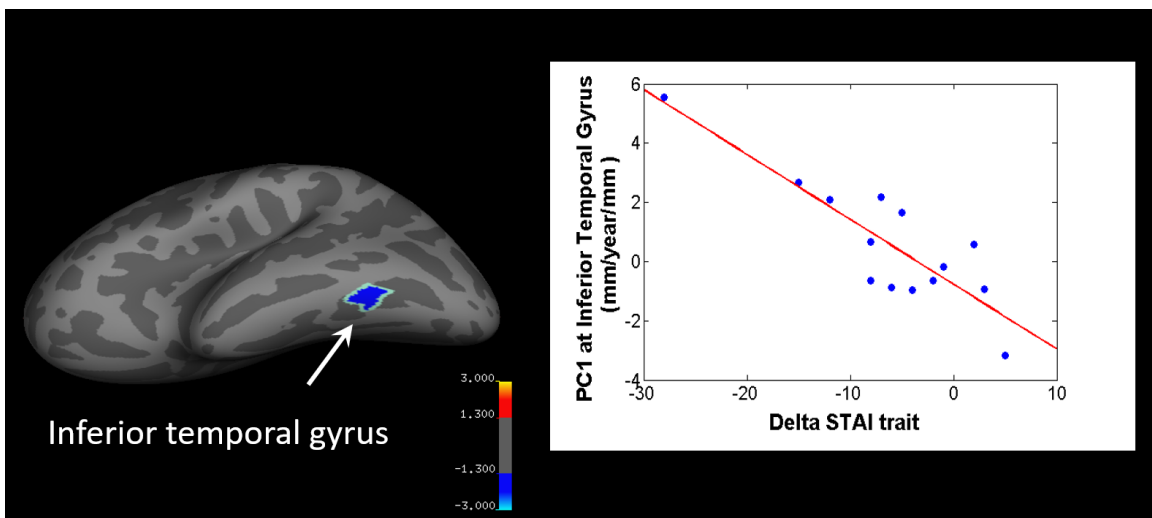


Figure 3.10: The STAI trait scores are negatively correlated with the percent thickness change in the left inferior temporal gyrus (Monte Carlo Simulation corrected.  $p<0.05$ ).  $r=-0.86$ ,  $p=0.001$ . Colorbar shows the false-positive rate ( $-\log_{10}(p)$ ): thresholds of -3, -1.3, 1.3, 3 correspond to  $p$ -values of -0.001, -0.05, 0.05, 0.001.[1]

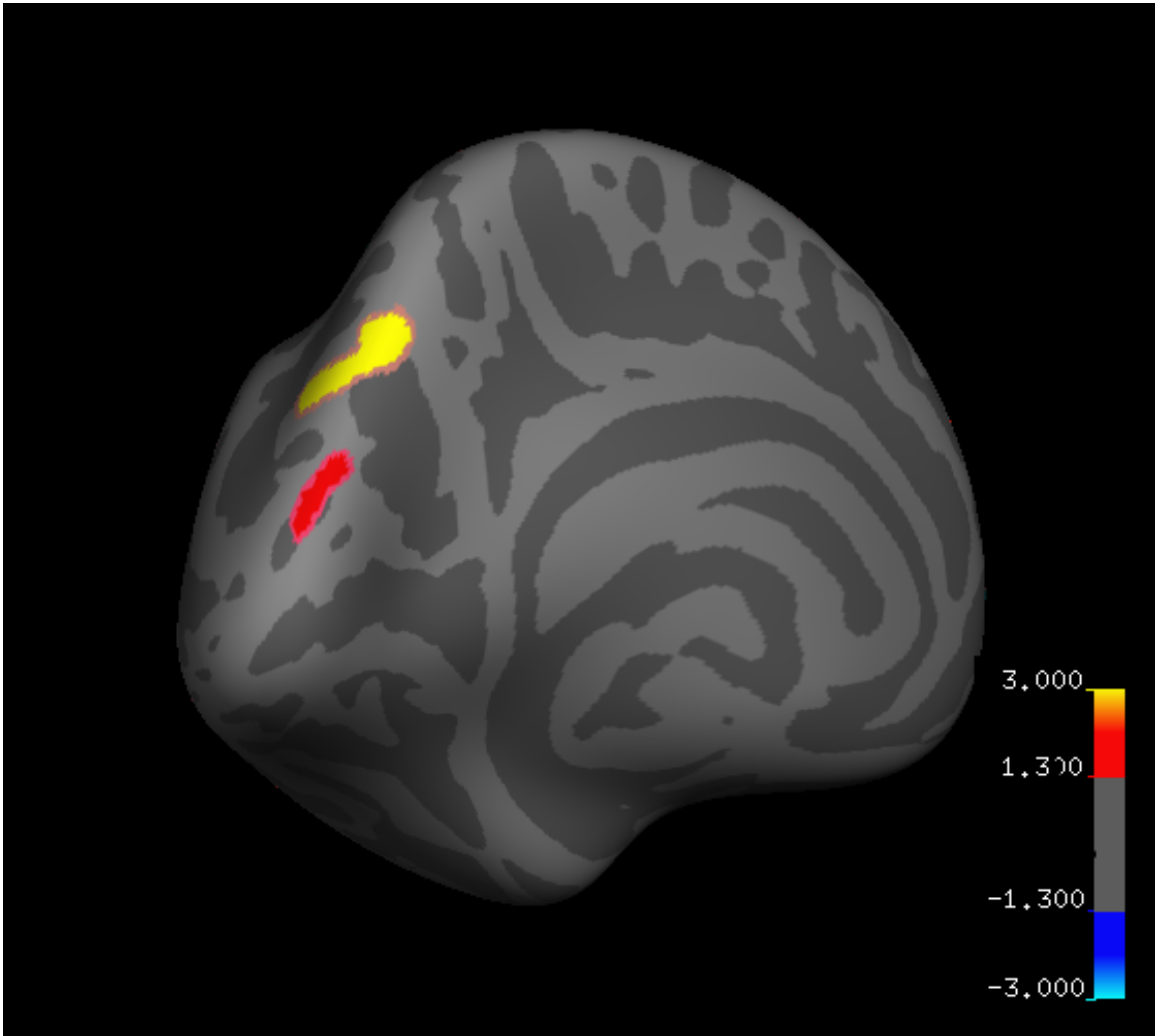


Figure 3.11: Whole brain pre-post cortical thickness changes (PC1: percent thickness change). Significant regional increases in cortical thickness following mindfulness meditation training in left precuneus (-12.7, -72.9, 40.7; shown in yellow) and left superior parietal lobule (-8.8, -89.2, 21.4; shown in red;  $p < 0.05$ , corrected by Monte Carlo simulation). Colorbar shows the false-positive rate ( $-\log_{10}(p)$ ): thresholds of -3, -1.3, 1.3, 3 correspond to p-values of -0.001, -0.05, 0.05, 0.001. [1]



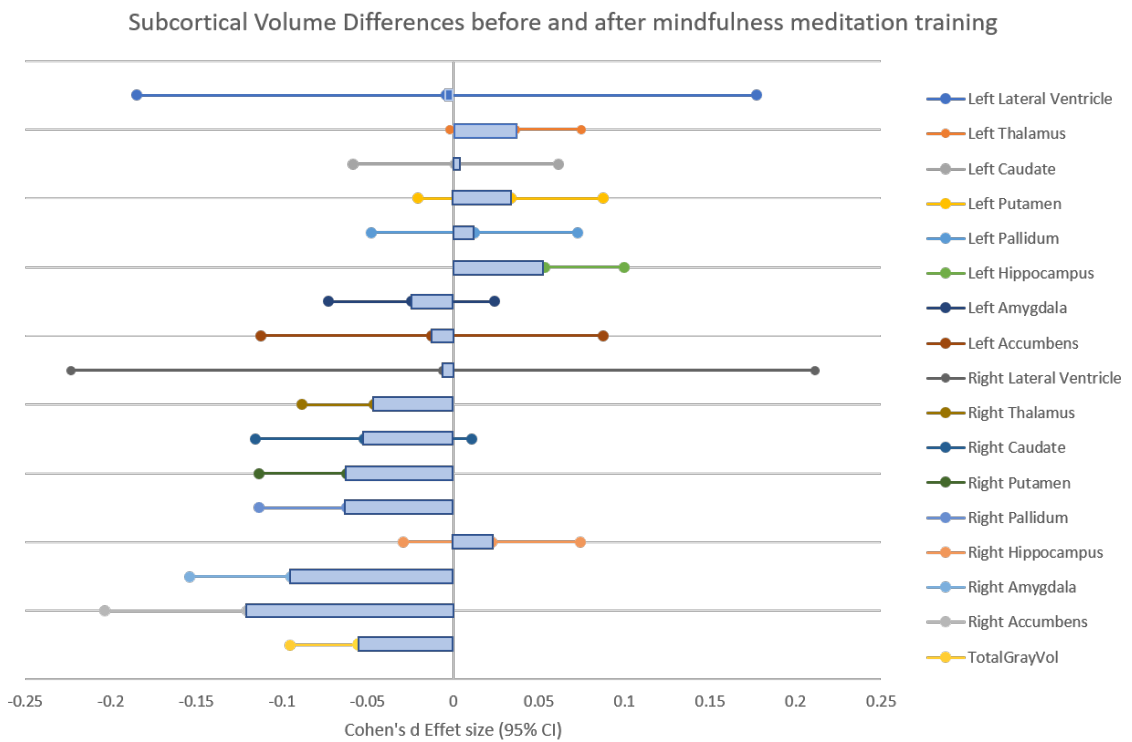


Figure 3.12: Subcortical volume differences before and after meditation training

Table 3.6: Summary of differences in subcortical volumes (mm<sup>3</sup>) of 16 brain regions between timepoints

<b>Brain regions</b>	<b>TP1 (n=14) Mean(SD)</b>	<b>TP2 (n=14) Mean (SD)</b>	<b>t</b>	<b>P-value<sup>a</sup></b>	<b>Cohens d</b>	<b>95% CI</b>
Left lateral ventricle	5868.69 (1914.95)	5859.47 (1854.80)	0.11	0.910	0.005	[-1003.09, 971.59]
Left thalamus	7948.70(569.46)	7929.07(597.88)	0.557	0.587	0.034	[-298.26, 313.21]
Left caudate	3944.92 (448.23)	3946.33 (467.69)	-0.116	0.909	-0.003	[-234.80, 244.98]
Left putamen	5735.78 (586.72)	5716.11 (587.88)	1.163	0.266	0.033	[-307.30, 307.98]
Left pallidum	2004.62 (236.29)	2001.97 (236.87)	0.332	0.745	0.011	[-123.76, 124.09]
Left hippocampus	4253.27 (371.16)	4234.51 (391.52)	0.789	0.444	0.049	[-194.37, 205.14]
Left amygdala	1463.10 (135.99)	1466.27 (136.77)	-0.317	0.756	-0.023	[-71.26, 71.62]
Left nucleus accumbens	509.92 (96.96)	509.91 (87.81)	0.001	0.999	0.0001	[-50.78, 46.00]
Right lateral ventricle	5538.62 (2066.03)	5517.83 (1945.68)	0.265	0.795	0.01	[-1082.22, 1019.20]
Right thalamus	7774.92 (628.02)	7798.32 (572.12)	-0.712	0.489	-0.039	[-329.01, 299.65]
Right caudate	3947.35 (466.16)	3971.22 (463.57)	-1.909	0.079	-0.051	[-244.24, 242.77]
Right putamen	5560.97 (533.67)	5594.37 (532.01)	-2.391	0.033	-0.063	[-279.61, 278.61]
Right pallidum	1979.15 (223.98)	1970.05 (233.02)	1.054	0.311	0.04	[-117.29, 122.10]
Right hippocampus	4308.62 (422.95)	4299.94 (432.14)	0.440	0.668	0.02	[-221.53, 226.38]
Right amygdala	1781.30 (194.52)	1795.00 (160.43)	-1.191	0.255	-0.078	[-101.97, 83.96]
Right nucleus accumbens	534.49 (89.03)	545.18 (92.43)	-1.913	0.078	-0.118	[-46.75, 48.30]

<sup>a</sup>Note: I report uncorrected p-values with a significance threshold determined by Bonferroni correction for testing 16 regions of interest (p=0.05/16=0.003).

## CHAPTER 4

### GENERAL DISCUSSION

#### 4.0.1 Summary of Findings across Modalities

##### *Summary - Functional Brain Imaging Results*

In the following section, the functional brain imaging results were summarized in [2]:

In the current study, I investigated longitudinal effects of mindfulness meditation training on changes in functional connectivity between brain areas. To our knowledge, no previous study has directly compared a meditation condition with a resting condition using sophisticated methods like ICA, ReHo, and FC. During the analyses, I specifically focused on target regions and resting state network playing a role in affective disorders like depression such as the pgACC, the dACC and the DMN. I found significant differences in functional connectivity both between states (rest vs. meditation) and between timepoints (pre- vs. post- training). The ICA analysis showed differences in the internal consistency in the precuneus and the temporo-parietal junction, increased during meditation, while the internal consistency of frontal brain regions decreased. The dACC further revealed reduced connectivity with anterior insula during meditation. As an indication of plastic changes following mindfulness meditation, reduced RSFC between the pgACC and dorsal medial prefrontal cortex was observed after meditation training.

##### *Summary - Structural Brain Imaging and ALFF Results*

In the following section, the structural brain imaging results as well as low-frequency amplitude results were summarized in [1]:

I investigated both the structural and ALFF changes following 40-days short-term mind-

fulness meditation training and their relationship with the mood effects of the practice. The results centred on the parietal cortex with a relative increase of cortical thickness in the left precuneus, which also importantly showed decreased ALFF. Further, these decreases were strongest for those subjects which also showed the most reductions in depression symptoms. Additional findings concerned the upper left parietal cortex and bilateral IPL, whereas cortical thickness increase in the left inferior temporal gyrus after meditation was correlated with STAI reductions after 40 days. For subcortical volume, I had observed the increase of volume in right putamen.

## **4.1 Discussion**

The psychometry findings and the functional imaging findings of the mindfulness meditation and its implication for the brain plasticity induction supporting the therapeutic efficacy were intensively discussed and linked to the framework of brain networks [2]:

### 4.1.1 Discussion Clinical

#### *Psychometry Findings*

Our findings indicate that the short-term practice of mindfulness meditation lead to differences in CES-D score before and after training. The nearly 50% reduction in depressive symptoms after mindfulness meditation training is consistent with recent meta-analyses reported by [54], [107]. Short-term meditation training yielded lowered acute feelings of tension at the time of scanning in our study. Likewise, our results emulate previous reports on the effects of meditation on well-being in anxiety trait and depression self-reports [108].

#### 4.1.2 Discussion - Functional Brain Imaging Results

##### *a. Imaging Findings*

ICA revealed that during MS, in comparison to RS, the DMN component had stronger association of TPJ and precuneus, while activity in frontal, cingulate and insular cortex was less associated with DMN. This may reflect the expected network dissociation as a function of cognitive task during meditation.

##### *b. Implication for Acute Effects and Plasticity Induction during Supporting Therapeutic Efficacy of Meditation*

The reported beneficial effects of mindfulness meditation for the treatment of emotional dysregulation in major depression and other affective disorders led us to hypothesize longitudinal changes in the RSFC. Changes in self-reports suggest that meditation training are very well in accordance with enduring changes in brain function as found in the literature [109], [5] and also in our study. In this sense, the longitudinal observation of RSFC decreases is very well in line with cross-sectional observations of altered functional responses [70] and RS connectivity, especially in the DMN. As one key region mediating depression-related symptoms, pgACC showed a longitudinal reduction in its connectivity with the PCC/precuneus region and conversely increased its connectivity with the right IPL. Such a reduction of intrinsic connectivity between pgACC and the posterior DMN components in precuneus would indeed reflect the expected directionality of connectivity changes if a hyperconnectivity within DMN in major depressive disorder (MDD), being considered a target of the antidepressant efficacy of meditation training. Sheline and colleagues [65] reported that such hyperconnectivity in the DMN exists for MDD; and in their study, they highlighted the importance of abnormal hyperconnectivity of a dorsal nexus. Quite consistently, I also found a reduction of connectivity between pgACC and dmPFC, close to the previously reported dorsal nexus region. That such changes of RSFC after in-

terventions of antidepressant action can also be observed in healthy subjects was recently supported by a finding from Scheidegger and colleagues [110], who showed that similar to our finding, a connectivity decrease of anterior and posterior DMN components, located in pgACC and PCC, was observed after 24hrs of ketamine injection, mirroring the substances' maximum antidepressant effects in patients. In other words, the neuronal effects observed after 40 days of meditation, which was shown to affect depression-related psychometry, also reduced connectivity in a network that is hyperconnected in MDD, and given the predominance of pgACC findings, this further suggests some specificity given the overall role of its dysfunction and abnormal connectivity in depression [74]. Longitudinal meditation training effects on functional connectivity are expected to be subserved by acute meditation effects when compared to resting conditions. Similar to the observed longitudinal reduction of RSFC between anterior and posterior DMN components I found an opposite pattern of connectivity changes from rest for pgACC compared to lateral and medial parietal DMN subcomponents. At the same time, the frontal DMN subcomponents seemed to aggregate as indicated by the increased RSFC between pgACC and dmPFC during meditation. Next to within network connectivities our results showed convergence of state (between conditions) and trait (between timepoints) effects on the alteration of the functional connectivity between pgACC and right TPJ. Here increased connectivities between these two regions would be in line with functional role of TPJ in reorienting of attention [111]. In the meditation technique applied here, both focused attention and open monitoring aspects were combined. While increased pgACC - TPJ connectivity very well fits together with an improvement of open monitoring behavior such as present moment awareness, it would equally well fit into potential antidepressant efficacy reversing narrowed or biased attention [75], although I did not include a direct measure of such behavioral effects.

When investigating the effects on the attention maintenance network [72], dACC was found to exert a reduced connectivity with its functional counterpart in the AI in MS compared to RS (Figure 3.2). Previous studies reported insula activity during meditation [36]

and anatomical changes in terms of increased gray matter [43][112]. The dACC region was however not found to show increased gray matter in either study. This structural distinction of subregions with and without volumetric differences within the cingulo-opercular network would be in line with our structural decoupling during meditation. In the literature there are also findings of increases in dACC activity, especially in expert meditators [113] and recent investigations of focused breathing versus mind wandering reported increased activation in both dACC and AI [21]. When interpreting our findings in line with functional involvements of dACC and AI, next to specifications of the explicit study design, one also has to acknowledge that one region can be part of several networks. This is especially true for AI, which next to its involvement in focused attention, together with dACC, is activated together with MPFC during self-referential conditions and further plays an important role in orchestrating different networks [114]. In contrast to the observed decoupling of AI and dACC in our seed-based analysis, the finding of reduced correlation with the DMN independent components of these two regions appears within a general observation of reduced IC connectivity in all task-positive regions (Figure 3.6). Here dACC and AI both showed similar effects of functional decoupling with DMN as an effect of differentiated task behavior during meditation, which however does not imply that they were necessarily any more functionally coupled. The differential effects on dACC and AI are also supported by the local metrics of the ReHo analysis. Here, the comparison between RS and MS conditions revealed increased ReHo during MS in the MPFC, the dACC and subcortical regions but not in insula cortices. Since this is the first paper to our knowledge to apply ReHo measures to resting or active states in meditators, one cannot directly relate our observations to other findings. When trying to relate changes of temporal synchrony [97] to cross sectional changes in patient populations, one likewise has to acknowledge that for MPFC both increases and decreases have been reported. While decreases have been for MPFC and ACC in depression [115], but also social anxiety [116] or Alzheimer disease [117], a recent study in bipolar depression rather indicated an increase of ReHo in MPFC [115]. If indeed the

functional distinction in increased versus decreased ReHo in bipolar versus MDD patients would mirror functional states that also discern rest versus active meditation, this would need to be subject to future investigations targeting the specificity and the physiological meaning of this observation. One important addition to the other connectivity-based findings is however provided by altered ReHo in putamen. This structure has been repeatedly reported in meditation studies [37], [118–120], but distinct from the other main regions frequently reported, was not revealed by our connectivity analyses.

#### 4.1.3 Discussion - ALFF and Structural Brain Imaging Results

Both the low frequency amplitude and structural brain imaging findings were in-depth discussed while linked to the previous literature as published in [2]:

Our findings of structural changes following the meditation training period confirmed our hypothesis about directionality based on previous results. In our study, greater thickness was observed in the left superior parietal cortex and left precuneus. A previous study demonstrated increased cortical thickness, but focuses on multiple prefrontal areas and insula regions [51]. In that study, however, the authors reported a cross-sectional increase with a long-term meditators cohort relative to meditation-naïve controls. In other cross-sectional studies, once again greater cortical thickness has been observed at the prefrontal cortex [43, 121] and in insula regions [43] for the meditation group compared to the matched controls. The focus of the effects on the parietal cortex, as found in our study, has to be considered in contrast to other studies. In principle, one may assume two major potential sources of this difference, one related to the investigated modalities and another to the varying experimental conditions. Most of the studies performed to date have used grey matter volumetric analyses which, in contrast to our cortical thickness measures, may have biased the findings; e.g. towards subcortical areas. However, thickness changes have also been reported that have also focused on prefrontal or insula areas. Particularly the



study by Santarnecchi et al. also applied MBSR training over 8 weeks, so the differences would have been considered minimal. Nevertheless in their study, no significant effects were found in the precuneus, but strong effects were noted in the insula and somatosensory cortices instead [47]. Furthermore, rather than using surface-based methods, those authors used voxel-based cortical thickness measures [47]. While the sources of varying structural changes in comparison to previous studies cannot be entirely identified, the current structural findings seem, however, plausible given their spatial overlap with accompanying functional changes. Our previous study showed functional brain changes by employing resting-state functional connectivity (RSFC) and regional homogeneity (ReHo) measures after short-term mindfulness meditation training [2]. Rs-fMRI has been extensively used in recent years for investigating the neural correlates associated with mindfulness meditation training [2, 29, 38, 122–124]. By employing ALFF measures in the present study, I found the decreased intensity of low-frequency oscillations in regions of the DMN (PCC/precuneus and bilateral IPL) after mindfulness training. Differential ALFF results have been observed in major depressive disorders (MDD) patients [125–127]. Increased ALFF in IPL has been found in MDD patients compared to healthy controls [127]. It is noteworthy that an rs-fMRI study by Sheline et al. has reported hyper-connectivity in the DMN for MDD subjects [65]. Other than in structural studies, the functional activity and connectivity of precuneus and superior parietal cortices are more frequently reported in meditation studies. The superior parietal cortex is related to attentional function developed during the practice of mindfulness meditation [122]. In the precuneus, self-referential processing is associated with increased functional activity [128], which decreases during mindful self-awareness [129]. Likewise, an altered RSFC of the superior parietal and precuneus has been observed in several previous meditation studies [2, 130, 131]. Superior parietal changes overlap with previously reported cortical thickness changes in Zen meditators [132]. Furthermore, these findings extend our prior work based on the same subjects, that FC during meditation practice increased in the precuneus when compared to the base-

line RSFC [2]. In a meta-analysis on the structural effects of meditation, the precuneus emerged as a region of structural heterogeneities in meditation practitioners [46]. Fox et al. suggested that the structural connectivity between the precuneus and areas of the attentional network, e.g. the superior parietal lobe, may be mediated by changes in the structural white matter at the superior longitudinal fasciculus after brief meditation training. Therefore, increments in cortical thickness in the superior parietal and precuneus after short-term meditation training may be caused by other structural changes in white matter connectivity as well as FC during the mindfulness state as a practice effect after brief mindfulness meditation.

Further, structural and functional changes were accompanied by reductions in depression scores and anxiety traits. To reveal an indication of the interrelation of behavioural and brain effects of meditation, I correlated the significant changes in the behavioural scores from the questionnaires (CES-D, STAI-trait) with brain changes in both dimensions. The precuneus was revealed in both structural and functional findings, and the PCC/precuneus also showed decreased ALFF, which correlated directly with the CES-D reductions. The relation between precuneus resting state behaviour and depression symptoms has been demonstrated in many studies, mostly in depressed cohorts [133, 134]. Here one could see that the PCC/precuneus, in its intrinsic fluctuation amplitudes, is also related to varying subclinical expressions of depressive symptomatology and their modulation by mindfulness meditation training, which has per se been demonstrated to act on depressive symptoms[135]. Interestingly, while the structural changes in the precuneus was observed, they did not correlate with the amount of CES-D reductions. Furthermore, no other region correlated with this effect at the whole brain level, which places the co-occurrence of the structural and functional findings in a more complex picture. One could interpret the divergence of correlations as being indicative of stronger, more sensitive effects in the functional domain. However, it is necessary to note that for the other behavioural effect, namely reduced anxiety, I found correlation with the thickness increases in the inferior temporal

Functional Changes	Structural Changes	Clinical Changes
<ul style="list-style-type: none"> <li>• Longitudinal decrease of RSFC of pgACC-precuneus, and pgACC-dmPFC (DMN decreases)</li> <li>• ALFF decreases at precuneus</li> </ul>	<ul style="list-style-type: none"> <li>• Increase of cortical thickness at precuneus</li> </ul>	<ul style="list-style-type: none"> <li>• Reduction of depression score (CES-D)</li> </ul>

Figure 4.1: Summary of main findings across modality

gyrus. Taken together, the longitudinal changes seemed to show a regional overlap in the precuneus, which in itself may indicate true neuronal effects observed across modalities, while their interindividual covariations with the behaviour consequences of mindfulness meditation training support the notion of a brain-wide network affected by the multitude of functional effects. Investigating this divergence and identifying the potential driving mechanisms may explain why effects on STAI reductions were found at different locations and in a distinct modality from that for the functional changes associated with CES-D.

#### 4.1.4 Discussion of Combination of Results from rs-fMRI / Structural MRI / Clinical

Here in this thesis, I found the reduced rsFC between pgACC and dmPFC, reduced rsFC between pgACC and the PCC/precuneus, as well as the increased rsFC between pgACC and right IPL as seen in Figure 4.2. The reduction of rsFC between pgACC and dmPFC which is near to dorsal nexus area. Importantly, in the study of Sheline et al. in 2010, they found abnormal hyperconnectivity of a dorsal nexus in MDD patients. Further, in Scheidegger et al. 2012, they used a single antidepressant dose of ketamine in healthy human subjects, and they found the reduction of rsFC of the dorsal nexus (DN) to the DMN as seen in Figure 4.3. Similarly, our RSFC results of using pgACC as seed is similar to the rsFC findings of MDD patients, as in MDD patients the hyperconnectivity of DMN is often observed. This

RSFC changes following mindfulness meditation training might imply the antidepressant efficacy of mindfulness meditation training (DMN decreases). Further, after the mindfulness training, the decreased intensity of ALFF in regions of the DMN (PCC/precuneus and bilateral IPL) were seen. Increased ALFF in IPL was found in previous study of MDD subjects compared to healthy controls [127]. The finding of ALFF decrease at PCC/precuneus within DMN alone with the findings of RSFC decrease of pgACC-PCC/precuneus (with in DMN) might indicate the antidepressant effect of the short-term mindfulness training, though further RCT studies which includes the control group is needed. At structural level, I observed cortical thickness increase at precuneus. Interestingly, the increase of cortical thickness and the reduction of ALFF was seen in precuneus, that both the structural and functional effects were found due to the practice of mindfulness meditation. Of note, I observed the reduction of ALFF in left precuneus/PCC is related with the decrease of the CES-D depression scores. The current findings of structural and functional changes after short-term meditation training resulted in precuneus, which is located at the posterior DMN area, might be plausible, although the origins of varying structural alterations when comparing with previous findings cannot be identified entirely.

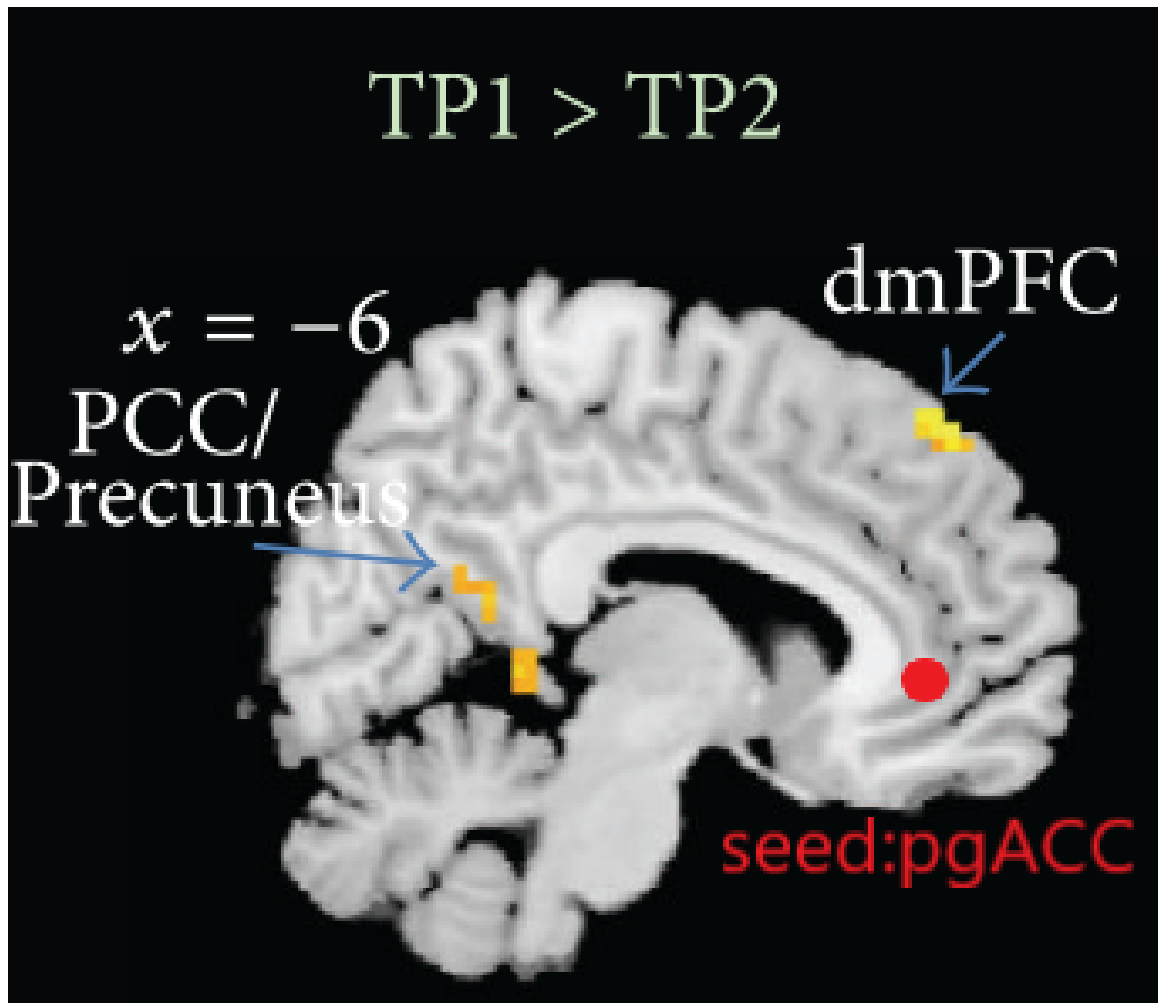


Figure 4.2: Longitudinal seed-based RSFC results (seed = pgACC) after 40 days of mindfulness meditation training ( $p < 0.05$ , FWE-corrected). A reduction of resting-state functional connectivity between pgACC and dmPFC, close to dorsal nexus region, was observed. [2]

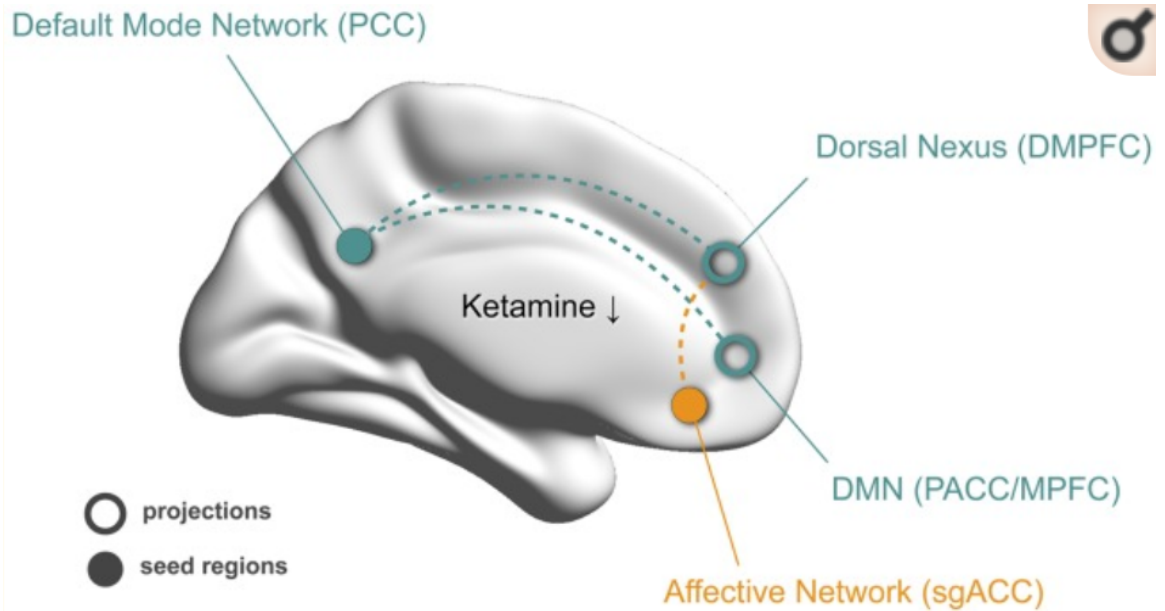


Figure 4.3: Proposed hypothetical model of ketamine-associated changes in functional connectivity. In the healthy human brain, a single antidepressant dose of ketamine reduces functional connectivity of the dorsal nexus (DN) to the Default Mode Network (DMN; green)<sup>2</sup>

<sup>2</sup>Reproduced from "Ketamine Decreases Resting State Functional Network Connectivity in Healthy Subjects: Implications for Antidepressant Drug Action", by Scheidegger et al, 2012, PLoS One, 2012, volume 7, issue 9, Copyright 2012 Scheidegger et al.

## CHAPTER 5

### CONCLUSION

#### 5.0.1 Summary

##### *Conclusion - Functional Brain Imaging Results*

To conclude, I observed reduction in depression-relevant symptoms also resting-state connectivity network changes after the 40-days mindfulness meditation training, which was normally observed in clinical studies such as in MDD patients as compared to healthy subjects. I found both longitudinal alterations as well as short-term effect when I directly compared the functional results between RS and MS. It was especially apparent when the cross-network interaction was observed at the regions of TPJ as well as AI. Within-network consistency was especially influenced in the DMN, that for both longitudinal and direct comparison of MS vs RS, the disconnection between anterior and posterior parts of DMN was observed. When comparing the condition between MS and RS, dACC decoupled from the DMN, this was overlapped spatially with the attention maintenance network [111], though the midcingulate cortex was also observed possibly due to individual variations in different data analysis steps and methods. The network effects as well as the local alteration of fluctuations, which might suggest specific effects in sub-areas of the salience network. This was especially subsidized by the reduction of functional connectivity between dACC and insula. Moreover, putamen was identified during meditation, which its local synchronization was increased. In sum, our functional brain findings contribute to our understanding of brain network related to the training of mindfulness meditation and provide a basis for its potential role of antidepressant efficacy.

### *Conclusion - ALFF and structural brain imaging results*

Our experiments confirmed that the short-term mindfulness meditation training reduced the subclinical depression symptomatology, which was also related to the reduction of low-frequency resting state fluctuations in the area of precuneus, where the cortical thickness was increased. This mechanism is parallel to the previous research on ALFF of depressed subjects and meditation, but more attention needs to be addressed to a network-wide effect while taking into account of the structural alteration in temporal areas and its changes in anxiety. Taken together, our findings of both functional and structural alterations offers valuable insights into the neural correlates of mindfulness meditation.

#### 5.0.2 Limitations

The generalisability of the findings is subject to certain limitations as in [2]:

Mindfulness meditation and its neural correlates have been investigated in several studies [136, 137] by means of block-design fMRI. A limitation of such a design is that meditation is difficult to perform with a short on-and-off period (30 - 45 sec), especially for novice meditators. This limitation also results from the GLM itself, in which a longer epoch will decrease the design efficiency. However, the study of Baerentsen et al., 2010, investigated continuous meditation by means of fMRI. They performed both SPM GLM and ICA on continuous meditation and focused on the difference between the meditation onset period and the maintained state of meditation. One may argue that independent component comparison still would best be performed for components identified across all conditions. In our case however, similar to Harrison et al 2008 who used a continuous sad mood induction paradigm compared to RS, I decided to decompose independent components for both conditions separately, also following the method of Calhoun et al 2008, who used ICASSO to insure ICA stability.

As I did not recruit a control group, the findings cannot be causally attributed solely



to mindfulness meditation so this will be an important improvement for future directions of further investigation. Moreover, the small sample size due to discarding of incomplete subjects and imaging artifacts due to motion inside the scanner, limits the generalizability of findings. An increased sample size will increase the statistical power in a future study. At baseline, the CES-D score of our sample slightly surpassed the clinical cut-off for depression (CES-D >16), which could be a potential selection bias. Despite a negative diagnosis of depression based on a personal interview, some of the participants may have had a subclinical depression. In this aspect, our sample may still be representative of the general population due to the high prevalence of subclinical depression in general population however inference to an entirely healthy population is limited. In our present study I did not collect physiological data. Future studies might consider inclusion of certain parameters, such as heart rate, breath rate and respiration amplitude. High-frequency heart rate variability (HF-HRV) is a measure of parasympathetic nervous system output that has been associated with enhanced self-regulation [120] would be of particular interest. Since meditation has been shown to increase HF-HRV, this might serve as a biomarker for meditation training-related effects. Recent findings however also suggest a direct relationship especially between HF-HRV and RSFC of e.g. cingulate regions [138], so that functional interpretation of connectivity changes could thus be directly related to autonomous nervous system tone. Further studies on MDD and other affective disorders may help to clarify the actual role of these changes in emotional regulation after short-term meditation, and its therapeutic effects.

Moreover, scrubbing was applied as the head motion regressor in functional data preprocessing step, in order to test the effect of the scrubbing itself on the data, analyses without using scrubbing was also carried out, which is provided in Appendix (see Appendix). I also supplied the pre- and post- head motion parameters (see Table B.3 and B.4 in Appendix).



# Appendices

## **APPENDIX A**

### **DATA PROCESSING**

In order to test the effect of scrubbing, I had performed ALFF analysis (without using scrubbing) during the preprocessing steps of functional brain data as published in the supplementary materials in [1]:

#### **A.1 ALFF analysis (with no scrubbing)**

I calculated ALFF by using DPARSF v 4.3. The time series for each voxel was fast Fourier-transformed (FFT) to acquire a power spectrum in the frequency domain. The square root of the power spectrum was obtained and averaged across a frequency of 0.01-0.1 Hz at each voxel. The averaged square root was thus known as ALFF. Further, the ALFF of each voxel for each participant was divided by the global mean ALFF for standardisation. Finally, the whole-brain-mean scaled ALFF maps were smoothed by applying a 6-mm full-width-at-half-maximum (FWHM) Gaussian kernel prior to the statistical analysis. Scrubbing was excluded as the deletion of time points breaks the temporal continuity of data and is not suitable for ALFF analysis.

#### **A.2 Statistical Analysis**

The voxel-wise ALFF analysis was performed to assess the whole brain amplitude of low-frequency fluctuations changes in mindfulness meditation training. A paired t-test was performed to test the whole brain longitudinal ALFF differences (two-tailed). Multiple comparisons were corrected at the FWE cluster level of  $p < 0.05$  with a conservative initial voxel height threshold of  $p < 0.001$ . A post hoc Pearson correlation analysis was also calculated to investigate the relation between the ALFF values and behavioural scores. As these

analyses were exploratory in nature, a statistical significance level of  $p < 0.05$  was used. The analysis was used with only those items from the questionnaires that revealed a significant main effect of intervention. Based on our behavioural results herein, the ALFF changes were correlated with the significant changes in the behavioural scores from questionnaires CES-D and STAI-trait.

## APPENDIX B

### ALFF RESULTS

The following section demonstrated the ALFF results without using scrubbing as in [1]:

#### B.1 The whole brain ALFF analysis result: ALFF changes after 40-days mindfulness meditation training

I found that ALFF decreased after meditation training at the left IPL, PCC/precuneus, middle temporal gyrus and MPFC ( $p < 0.05$ , FWE-corrected, Supplementary Figure B.1).

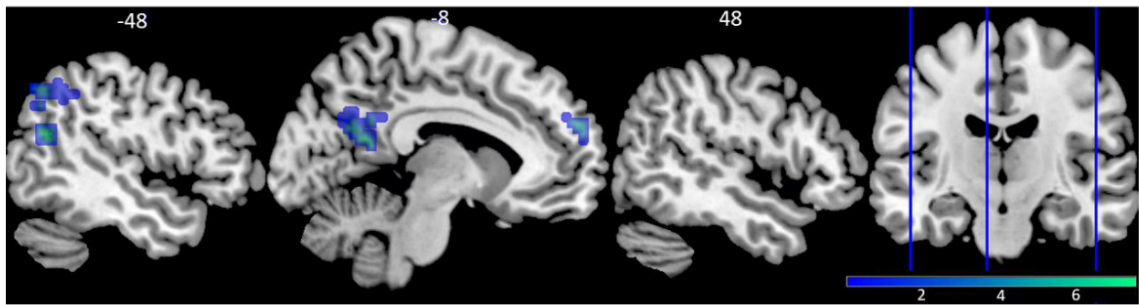


Figure B.1: Longitudinal ALFF decreased after mindfulness meditation training (TP1 Rest > TP2 Rest): Left IPL (left angular gyrus,  $-42, -60, 45; t = 5.97$ ), PCC/precuneus ( $6, -63, 27; t = 8.57$ ), middle temporal gyrus ( $-45, -60, 21; t = 9.34$ ) and MPFC ( $-9, 57, 27; t = 5.75$ ) were found. No correlations of behavioural scores were observed. [1]

#### B.2 Post hoc correlation analysis results

Correlations between the whole brain ALFF with significantly changing behavioural scores (CES-D, STAI-trait) were performed. There was no whole-brain corrected correlation of the meditation-induced changes and changes in the behavioural scores. Given the regional effects on PCC/precuneus, I extracted the delta mean ALFF values at PCC/precuneus and correlated these with the delta CES-D and delta STAI-trait scores, respectively. No correlations of behavioural scores were observed. Likewise, no significant correlations with

these variables were found at the baseline ALFF. In Supplementary Table B.3 and B.4, the pre- (TP1) and post-(TP2) head motion parameters are provided, and the translation and rotation information and the FD values are listed.

**Paired Samples Statistics**

		Mean	N	Std. Deviation	Std. Error Mean
Pair 1	mean_FD_power_TP1	.1828	13	.05191	.01440
	mean_FD_power_TP2	.1572	13	.05205	.01444

**Paired Samples Test**

		Paired Differences					t	df	Sig. (2-tailed)
		Mean	Std. Deviation	Std. Error Mean	95% Confidence Interval of the Difference				
					Lower	Upper			
Pair 1	mean_FD_power_TP1 - mean_FD_power_TP2	.02569	.06224	.01726	-.01192	.06330	1.488	12	.162

Figure B.2: The frame-wise displacement value (FD\_Power) showed no significant difference between the time points (t=1.488, p=0.162) [1]

TP	Subject	mean(abs(Tx))	mean(abs(Ty))	mean(abs(Tz))	mean(abs(Rx))	mean(abs(Ry))	mean(abs(Rz))	mean RMS	mean relative RMS (mean FD_VanDijk)	mean FD_Power	Number of FD_Power>0.5	Percent of FD_Power>0.5
	sub3	0.0151983	0.07273802	0.1809405	0.04480527	0.03665587	0.04357895	0.1986725	0.02547175	0.1155779	4	0.01793722
	sub5	0.01409969	0.06544304	0.04835991	0.05569284	0.08225464	0.05139342	0.09030822	0.03202484	0.1419358	2	0.00896861
	sub7	0.02236215	0.05784394	0.1290654	0.05501336	0.04318846	0.05071814	0.1500372	0.0405811	0.1847159	6	0.02690583
	sub8	0.02167207	0.11079612	0.2114903	0.06641303	0.04147747	0.06100735	0.2418854	0.04291214	0.1639321	9	0.04035874
	sub12	0.02839788	0.05476167	0.0802863	0.0405415	0.05048683	0.05231052	0.109452	0.04781977	0.2136102	4	0.01793722
	sub14	0.01971385	0.08628262	0.1160828	0.1054857	0.02689664	0.08749514	0.1515958	0.03710793	0.1744266	12	0.05381166
	sub15	0.01628963	0.09379231	0.09320236	0.0902286	0.03574942	0.03838046	0.1414177	0.0324727	0.1750566	16	0.07174888
	sub17	0.02571213	0.05907959	0.1176643	0.113068	0.03520642	0.03856588	0.1458289	0.04308352	0.1945846	6	0.02690583
	sub18	0.02022622	0.04874388	0.06141207	0.06093529	0.08205073	0.05779998	0.09055626	0.02569603	0.1917711	8	0.03587444
	sub21	0.03046562	0.11378536	0.1993605	0.0627382	0.05788174	0.04845473	0.2486094	0.03964463	0.1685577	6	0.02690583
	sub22	0.03234156	0.06289352	0.1092133	0.09995231	0.03702078	0.1132825	0.1406438	0.07541092	0.3299748	38	0.1704036
	sub23	0.01532091	0.05783718	0.03818827	0.04978103	0.05421904	0.02229377	0.07629214	0.05734548	0.1906727	9	0.04035874
	sub26	0.02232888	0.07088732	0.1590653	0.05606171	0.04331838	0.0289808	0.1799266	0.03573045	0.1321826	3	0.01345291

Figure B.3: Head motion parameters, and the translation and rotation information and the FD values at TP1



TP	Subject	mean(abs(Tx))	mean(abs(Ty))	mean(abs(Tz))	mean(abs(Rx))	mean(abs(Ry))	mean(abs(Rz))	mean RMS	mean relative RMS (mean FD_VanDijk)	mean FD_Power	Number of FD_Power>0.5	Percent of FD_Power>0.5
2	ID											
	sub3	0.01539552	0.03478931	0.05138207	0.05197914	0.06700348	0.03541032	0.06742325	0.01344869	0.0728512	0	0
	sub5	0.01812462	0.05690424	0.05060574	0.08261732	0.03934961	0.03626015	0.08765652	0.04128302	0.218802	21	0.0941704
	sub7	0.03078545	0.07007352	0.1293621	0.1768892	0.0867019	0.04845887	0.1560144	0.02070438	0.1166197	1	0.004484305
	sub8	0.01582044	0.04621254	0.06078308	0.02740242	0.04297189	0.04497996	0.08219848	0.02044382	0.1030081	1	0.004484305
	sub12	0.0253662	0.07370546	0.102986	0.07386375	0.05692132	0.05133243	0.1393431	0.04655124	0.2294676	7	0.03139013
	sub14	0.01699523	0.1095702	0.1047364	0.05103749	0.03555276	0.03425994	0.1581724	0.03756434	0.1586316	12	0.05381166
	sub15	0.01700554	0.05077497	0.08818791	0.06414983	0.03636336	0.03996101	0.1103746	0.03849127	0.2069613	22	0.09865471
	sub17	0.03174098	0.09882186	0.1554137	0.09652759	0.08153439	0.07893983	0.1922013	0.01974875	0.1100464	0	0
	sub18	0.02509003	0.0967653	0.06109133	0.07746879	0.04166638	0.03899126	0.1290893	0.05473764	0.2175229	8	0.03587444
	sub21	0.03444302	0.02587306	0.0554224	0.05893781	0.04865121	0.04134564	0.07899936	0.03178182	0.1711262	7	0.03139013
	sub22	0.01497928	0.07248993	0.1357867	0.06164489	0.04233907	0.03608474	0.1586662	0.04329636	0.1611382	7	0.03139013
	sub23	0.009044006	0.0530499	0.03526105	0.07179832	0.02623241	0.019063	0.07265462	0.0416927	0.1740319	3	0.01345291
	sub26	0.026864	0.02434812	0.1300451	0.04846036	0.01791987	0.05473478	0.1379966	0.02631477	0.1027692	3	0.01345291

Figure B.4: Head motion parameters, and the translation and rotation information and the FD values at TP2 [1]

## REFERENCES

1. Yang, C.-C. *et al.* Alterations in Brain Structure and Amplitude of Low-frequency after 8 weeks of Mindfulness Meditation Training in Meditation-Naïve Subjects. *Scientific Reports* **9**, 10977 (2019).
2. Yang, C.-c. *et al.* State and Training Effects of Mindfulness Meditation on Brain Networks Reflect Neuronal Mechanisms of Its Antidepressant Effect. *Neural Plasticity* **2016**, 1–14 (2016).
3. Kabat-Zinn, J. & Clinic, U. o. M. M. C. S. R. *Full Catastrophe Living: Using the Wisdom of Your Body and Mind to Face Stress, Pain, and Illness* ISBN: 9780385303125 (Delta Trade Paperbacks, 1990).
4. Pagnini, F. & Philips, D. *Being mindful about mindfulness* 2015.
5. Slagter, H. A., Davidson, R. J. & Lutz, A. Mental Training as a Tool in the Neuroscientific Study of Brain and Cognitive Plasticity. *Frontiers in Human Neuroscience* **5** (2011).
6. Siegel, D. J. Mindfulness training and neural integration: Differentiation of distinct streams of awareness and the cultivation of well-being. *Social Cognitive and Affective Neuroscience* (2007).
7. Bowen, S. *et al.* Mindfulness-based relapse prevention for substance use disorders: A pilot efficacy trial. *Substance Abuse* (2009).
8. Rosenzweig, S. *et al.* Mindfulness-based stress reduction for chronic pain conditions: Variation in treatment outcomes and role of home meditation practice. *Journal of Psychosomatic Research* (2010).
9. Garland, E. L., Gaylord, S. A., Boettiger, C. A. & Howard, M. O. Mindfulness training modifies cognitive, affective, and physiological mechanisms implicated in alcohol dependence: Results of a randomized controlled pilot trial. *Journal of Psychoactive Drugs* (2010).
10. Hölzel, B. K. *et al.* Neural mechanisms of symptom improvements in generalized anxiety disorder following mindfulness training. *NeuroImage: Clinical* **2**, 448–458 (2013).
11. Mindful America: the mutual transformation of Buddhist meditation and American culture. *Choice Reviews Online* (2015).

12. Davids, T. W. R. *Buddhist Suttas* (Clarendon Press, 1900).
13. Deepeshwar, S., Nagendra, H. R. & Rana, B. B. in *Progress in Brain Research* (2019). ISBN: 9780444642271.
14. Davidson, R. J. & Lutz, A. Buddha's Brain: Neuroplasticity and Meditation. *IEEE Signal Processing Magazine* **25**, 172–176 (2008).
15. Pascual-Leone, A. *et al.* Characterizing brain cortical plasticity and network dynamics across the age-span in health and disease with TMS-EEG and TMS-fMRI. *Brain Topography* (2011).
16. Holtmaat, A. & Caroni, P. *Functional and structural underpinnings of neuronal assembly formation in learning* 2016.
17. Zieliński, K. *Jerzy Konorski on brain associations* 2006.
18. Biswal, B., Zerrin Yetkin, F., Haughton, V. M. & Hyde, J. S. Functional connectivity in the motor cortex of resting human brain using echodffdfdfdfplanar mri. *Magnetic Resonance in Medicine* (1995).
19. Fox, M. D. & Raichle, M. E. *Spontaneous fluctuations in brain activity observed with functional magnetic resonance imaging* 2007.
20. Greicius, M. D. *et al.* Resting-State Functional Connectivity in Major Depression: Abnormally Increased Contributions from Subgenual Cingulate Cortex and Thalamus. *Biological psychiatry* **62**, 429–437 (Sept. 2007).
21. Menon, V. & Uddin, L. Q. *Saliency, switching, attention and control: a network model of insula function.* 2010.
22. Sridharan, D., Levitin, D. J. & Menon, V. A critical role for the right fronto-insular cortex in switching between central-executive and default-mode networks. **105**, 12569–12574 (2008).
23. Seeley, W. W. *et al.* Dissociable intrinsic connectivity networks for salience processing and executive control. *Journal of Neuroscience* **27**, 2349–2356 (2007).
24. Menon, V. *Large-scale brain networks and psychopathology: A unifying triple network model* 2011.
25. Luo, X. *et al.* Disrupted Cerebellar Connectivity With the Central Executive Network and the Default-Mode Network in Unmedicated Bipolar II Disorder. *Frontiers in Psychiatry* **9**, 1–10 (2018).

26. Levin, R. L., Heller, W., Mohanty, A., Herrington, J. D. & Miller, G. A. *Cognitive deficits in depression and functional specificity of regional brain activity* 2007.
27. Raichle, M. E. *et al.* A default mode of brain function. *Proceedings of the National Academy of Sciences of the United States of America* (2001).
28. Mars, R. B. *et al.* On the relationship between the "default mode network" and the "social brain". *Frontiers in Human Neuroscience* (2012).
29. Taylor, V. A. *et al.* Impact of meditation training on the default mode network during a restful state. *Social Cognitive and Affective Neuroscience* (2013).
30. Ashburner, J. & Friston, K. J. Voxel-Based Morphometry The Methods. *NeuroImage* **11**, 805–821 (2000).
31. Fischl, B. *et al.* Automatically Parcellating the Human Cerebral Cortex. *Cerebral Cortex* **14**, 11–22 (2004).
32. Fischl, B. & Dale, A. M. Measuring the thickness of the human cerebral cortex from magnetic resonance images. *Proceedings of the National Academy of Sciences* **97**, 11050–11055 (2000).
33. Kang, D. H. *et al.* The effect of meditation on brain structure: Cortical thickness mapping and diffusion tensor imaging. *Social Cognitive and Affective Neuroscience* **8**, 27–33 (2013).
34. Yang, H. *et al.* Neurochemical and neuroanatomical plasticity following memory training and yoga interventions in older adults with mild cognitive impairment. *Frontiers in Aging Neuroscience* **8**, 1–9 (2016).
35. Brewer, J. A. *et al.* Meditation experience is associated with differences in default mode network activity and connectivity. *Proceedings of the National Academy of Sciences* **108**, 20254–20259 (2011).
36. Lutz, A., Brefczynski-Lewis, J., Johnstone, T. & Davidson, R. J. Regulation of the neural circuitry of emotion by compassion meditation: Effects of meditative expertise. *PLoS ONE* (2008).
37. Brefczynski-Lewis, J. A., Lutz, A., Schaefer, H. S., Levinson, D. B. & Davidson, R. J. Neural correlates of attentional expertise in long-term meditation practitioners. *Proceedings of the National Academy of Sciences of the United States of America* (2007).
38. Jang, J. H. *et al.* Increased default mode network connectivity associated with meditation. *Neuroscience Letters* **487**, 358–362 (2011).

39. Hölzel, B. K. *et al.* Mindfulness practice leads to increases in regional brain gray matter density. *Psychiatry Research - Neuroimaging* (2011).
40. Davanger, S., Ellingsen, O., Holen, A. & Hugdahl, K. Meditation-specific prefrontal cortical activation during acem meditation: an fMRI study. *Perceptual and motor skills* **111**, 291–306 (2010).
41. Farb, N. A., Segal, Z. V. & Anderson, A. K. Mindfulness meditation training alters cortical representations of interoceptive attention. *Social Cognitive and Affective Neuroscience* **8**, 15–26 (2013).
42. Hölzel, B. K. *et al.* Mindfulness practice leads to increases in regional brain gray matter density. *Psychiatry Research: Neuroimaging* (2010).
43. Lazar, S. W. *et al.* Meditation experience is associated with increased cortical thickness. *NeuroReport* **16**, 1893–1897 (2005).
44. Zang, Y. F. *et al.* Altered baseline brain activity in children with ADHD revealed by resting-state functional MRI. *Brain and Development* **29**, 83–91 (2007).
45. Lu, H. *et al.* Synchronized delta oscillations correlate with the resting-state functional MRI signal. *Proceedings of the National Academy of Sciences* (2007).
46. Fox, K. C. R. *et al.* *Is meditation associated with altered brain structure? A systematic review and meta-analysis of morphometric neuroimaging in meditation practitioners* 2014.
47. Santarnecchi, E. *et al.* Interaction between neuroanatomical and psychological changes after mindfulness-based training. *PLoS ONE* **9**, 1–9 (2014).
48. Pickut, B. A. *et al.* Mindfulness based intervention in Parkinson's disease leads to structural brain changes on MRI: A randomized controlled longitudinal trial. *Clinical Neurology and Neurosurgery* **115**, 2419–2425 (2013).
49. Tang, Y.-y. *et al.* Short-term meditation induces white matter changes in the anterior cingulate. **107**, 15649–15652 (2010).
50. Hernández, S. E., Barros-Loscertales, A., Xiao, Y., González-Mora, J. L. & Rubia, K. Gray Matter and Functional Connectivity in Anterior Cingulate Cortex are Associated with the State of Mental Silence During Sahaja Yoga Meditation. *Neuroscience* **371**, 395–406 (2018).
51. Engen, H. G., Bernhardt, B. C., Skottnik, L., Ricard, M. & Singer, T. Structural changes in socio-affective networks: Multi-modal MRI findings in long-term meditation practitioners. *Neuropsychologia* (2017).

52. Chambers, R., Gullone, E. & Allen, N. B. *Mindful emotion regulation: An integrative review* 2009.
53. Farb, N. A., Anderson, A. K. & Segal, Z. V. *The mindful brain and emotion regulation in mood disorders* 2012.
54. Hofmann, S. G., Sawyer, A. T., Witt, A. A. & Oh, D. The Effect of Mindfulness-Based Therapy on Anxiety and Depression: A Meta-Analytic Review. *Journal of Consulting and Clinical Psychology* (2010).
55. Hölzel, B. K. *et al.* How Does Mindfulness Meditation Work? Proposing Mechanisms of Action From a Conceptual and Neural Perspective. *Perspectives on Psychological Science* **6**, 537–559 (Oct. 2011).
56. Tang, Y. Y. & Posner, M. I. *Special issue on mindfulness neuroscience* 2013.
57. Ramel, W., Goldin, P. R., Carmona, P. E. & McQuaid, J. R. The effects of mindfulness meditation on cognitive processes and affect in patients with past depression. *Cognitive Therapy and Research* (2004).
58. Goyal, M. *et al.* Meditation programs for psychological stress and well-being : a systematic review and meta-analysis. *JAMA Intern Med* **174**, 357–68 (2014).
59. Marchand, W. R. Neural mechanisms of mindfulness and meditation: Evidence from neuroimaging studies. *World Journal of Radiology* **6**, 471 (2014).
60. Mars, T. S. & Abbey, H. Mindfulness meditation practise as a healthcare intervention: A systematic review. *International Journal of Osteopathic Medicine* (2010).
61. Hilton, L. *et al.* Mindfulness Meditation for Chronic Pain: Systematic Review and Meta-analysis. *Annals of Behavioral Medicine* (2017).
62. Lopez-Maya, E., Olmstead, R. & Irwin, M. R. Mindfulness meditation and improvement in depressive symptoms among Spanish- and English speaking adults: A randomized, controlled, comparative efficacy trial. *PLOS ONE* (2019).
63. Black, D. S., O'Reilly, G. A., Olmstead, R., Breen, E. C. & Irwin, M. R. Mindfulness meditation and improvement in sleep quality and daytime impairment among older adults with sleep disturbance: A randomized clinical trial. *JAMA Internal Medicine* **175** (2015).
64. Saeed, S. A., Antonacci, D. J. & Bloch, R. M. Exercise, yoga, and meditation for depressive and anxiety disorders. *American Family Physician* (2010).

65. Sheline, Y. I., Price, J. L., Yan, Z. & Mintun, M. A. Resting-state functional MRI in depression unmasks increased connectivity between networks via the dorsal nexus. *Proceedings of the National Academy of Sciences* (2010).
66. Gusnard, D. A., Akbudak, E., Shulman, G. L. & Raichle, M. E. Medial prefrontal cortex and self-referential mental activity: Relation to a default mode of brain function. *Proceedings of the National Academy of Sciences of the United States of America* (2001).
67. Ochsner, K. N. & Gross, J. J. *The cognitive control of emotion* 2005.
68. Lemogne, C. *et al.* In search of the depressive self: Extended medial prefrontal network during self-referential processing in major depression. *Social Cognitive and Affective Neuroscience* (2009).
69. Berman, M. G. *et al.* Depression, rumination and the default network. *Social Cognitive and Affective Neuroscience* (2011).
70. Walter, M., Henning, A., Grimm, S. & al et, e. THE relationship between aberrant neuronal activation in the pregenual anterior cingulate, altered glutamatergic metabolism, and anhedonia in major depression. *Archives of General Psychiatry* **66**, 478–486 (May 2009).
71. Bush, G., Luu, P. & Posner, M. I. *Cognitive and emotional influences in anterior cingulate cortex* 2000.
72. Dosenbach, N. U., Fair, D. A., Cohen, A. L., Schlaggar, B. L. & Petersen, S. E. A dual-networks architecture of top-down control. *Trends in Cognitive Sciences* (2008).
73. Van Tol, M. J. *et al.* Regional brain volume in depression and anxiety disorders. *Archives of General Psychiatry* (2010).
74. Horn, D. I. *et al.* Glutamatergic and Resting-State Functional Connectivity Correlates of Severity in Major Depression fffdfdfdf The Role of Pregenual Anterior Cingulate Cortex and Anterior Insula. *Frontiers in Systems Neuroscience* **4**, 33 (July 2010).
75. Disner, S. G., Beevers, C. G., Haigh, E. A. & Beck, A. T. *Neural mechanisms of the cognitive model of depression* 2011.
76. Kaiser, R. H., Andrews-Hanna, J. R., Wager, T. D. & Pizzagalli, D. A. Large-Scale Network Dysfunction in Major Depressive Disorder. *JAMA Psychiatry* (2015).
77. Smith, S. M. *et al.* Network modelling methods for FMRI. *NeuroImage* (2011).

78. Baer, R. A., Smith, G. T., Hopkins, J., Krietemeyer, J. & Toney, L. Using Self-Report Assessment Methods to Explore Facets of Mindfulness. *Assessment* **13**, 27–45 (2006).
79. Hayes, S. C. *et al.* Acceptance and commitment therapy: model, processes and outcomes. *Behaviour research and therapy* **44**, 1–25 (2006).
80. Andrade, E. *et al.* Factor structure and invariance of the POMS Mood State Questionnaire in Spanish. *The Spanish journal of psychology* **13**, 444–452 (2010).
81. McNair, D., Lorr, M. & Droppleman, L. *EDITS manual for the profile of mood states*. 40 (1971).
82. Radloff, L. S. The CES-D Scale: A Self-Report Depression Scale for Research in the General Population. *Applied Psychological Measurement* **1**, 385–401 (1977).
83. Spielberger, C. D., Gorsuch, R. L., Lushene, P. R., Vagg, P. R. & Jacobs, A. G. *Manual for the State-Trait Anxiety Inventory (Form Y)* 4–6. ISBN: 978-1-4419-9892-7 (1983).
84. Dale, A. M., Fischl, B. & Sereno, M. I. Cortical surface-based analysis: I. Segmentation and surface reconstruction. *NeuroImage* **9**, 179–194 (1999).
85. Smith, S. M. *et al.* *Advances in functional and structural MR image analysis and implementation as FSL in NeuroImage* **23** (2004). ISBN: 1053-8119 (Print).
86. Yan. DPARSF: a MATLAB toolbox for fMRI data analysis of resting-state fMRI. *Frontiers in System Neuroscience* **4**, 1–7 (2010).
87. Lowe, M. J., Mock, B. J. & Sorenson, J. A. Functional connectivity in single and multislice echoplanar imaging using resting-state fluctuations. *NeuroImage* (1998).
88. Murphy, K., Birn, R. M., Handwerker, D. A., Jones, T. B. & Bandettini, P. A. The impact of global signal regression on resting state correlations: Are anti-correlated networks introduced? *NeuroImage* (2009).
89. Price, J. L. & Drevets, W. C. *Neurocircuitry of mood disorders* 2010.
90. Lord, A., Horn, D., Breakspear, M. & Walter, M. Changes in community structure of resting state functional connectivity in unipolar depression. *PLoS ONE* (2012).
91. Calhoun, V. D., Adali, T., Pearlson, G. D. & Pekar, J. J. A method for making group inferences from functional MRI data using independent component analysis. *Human Brain Mapping* **14**, 140–151 (Nov. 2001).



92. Chen, S. *et al.* Group independent component analysis reveals consistent resting-state networks across multiple sessions. *Brain Research* (2008).
93. Calhoun, V. D., Kiehl, K. A. & Pearlson, G. D. Modulation of temporally coherent brain networks estimated using ICA at rest and during cognitive tasks. *Human Brain Mapping* (2008).
94. Harrison, B. J. *et al.* Modulation of brain resting-state networks by sad mood induction. *PLoS ONE* (2008).
95. Bell, A. J. & Sejnowski, T. J. The 'independent components' of natural scenes are edge filters. *Vision Research* (1997).
96. Kendall, M. G. & Gobbons, J. D. *Rank Correlation Methods* 272. ISBN: 0195208374 (1990).
97. Zang, Y., Jiang, T., Lu, Y., He, Y. & Tian, L. Regional homogeneity approach to fMRI data analysis. *NeuroImage* (2004).
98. Yan, C. G., Wang, X. D., Zuo, X. N. & Zang, Y. F. DPABI: Data Processing & Analysis for (Resting-State) Brain Imaging. *Neuroinformatics* **14**, 339–351 (2016).
99. Yan, C. G. *et al.* A comprehensive assessment of regional variation in the impact of head micromovements on functional connectomics. *NeuroImage* (2013).
100. Fischl, B. *et al.* Whole brain segmentation: Automated labeling of neuroanatomical structures in the human brain. *Neuron* **33**, 341–355 (2002).
101. Fischl, B., Liu, A. & Dale, A. M. Automated manifold surgery: Constructing geometrically accurate and topologically correct models of the human cerebral cortex. *IEEE Transactions on Medical Imaging* **20**, 70–80 (2001).
102. Ségonne, F., Pacheco, J. & Fischl, B. Geometrically accurate topology-correction of cortical surfaces using nonseparating loops. *IEEE Transactions on Medical Imaging* **26**, 518–529 (2007).
103. Destrieux, C., Fischl, B., Dale, A. & Halgren, E. Automatic parcellation of human cortical gyri and sulci using standard anatomical nomenclature. *NeuroImage* **53**, 1–15 (2010).
104. Reuter, M., Rosas, H. D. & Fischl, B. Highly accurate inverse consistent registration: A robust approach. *NeuroImage* (2010).
105. Reuter, M., Schmansky, N. J., Rosas, H. D. & Fischl, B. Within-subject template estimation for unbiased longitudinal image analysis. *NeuroImage* (2012).

106. Reuter, M. & Fischl, B. *Avoiding asymmetry-induced bias in longitudinal image processing* 2011.
107. Vibe, M., Bjørndal, A., Tipton, E., Hammerstrøm, K. & Kowalski, K. Mindfulness Based Stress Reduction (MBSR) for Improving Health, Quality of Life, and Social Functioning in Adults. *Campbell Systematic Reviews* (2012).
108. Shapiro, S. L., Schwartz, G. E. & Bonner, G. Effects of mindfulness-based stress reduction on medical and premedical students. *Journal of Behavioral Medicine* (1998).
109. Desbordes, G. *et al.* Effects of mindful-attention and compassion meditation training on amygdala response to emotional stimuli in an ordinary, non-meditative state. *Frontiers in Human Neuroscience* (2012).
110. Scheidegger, M. *et al.* Ketamine Decreases Resting State Functional Network Connectivity in Healthy Subjects: Implications for Antidepressant Drug Action. *PLoS ONE* (2012).
111. Dosenbach, N. U. *et al.* Distinct brain networks for adaptive and stable task control in humans. *Proceedings of the National Academy of Sciences of the United States of America* (2007).
112. Hölzel, B. K. *et al.* Differential engagement of anterior cingulate and adjacent medial frontal cortex in adept meditators and non-meditators. *Neuroscience Letters* (2007).
113. Lutz, A., Greischar, L. L., Perlman, D. M. & Davidson, R. J. BOLD signal in insula is differentially related to cardiac function during compassion meditation in experts vs. novices. *NeuroImage* (2009).
114. Liu, C. H. *et al.* Regional Homogeneity within the Default Mode Network in Bipolar Depression: A Resting-State Functional Magnetic Resonance Imaging Study. *PLoS ONE* (2012).
115. Qiu, C. *et al.* Regional homogeneity changes in social anxiety disorder: A resting-state fMRI study. *Psychiatry Research - Neuroimaging* (2011).
116. Zhang, Z. *et al.* Altered spontaneous activity in Alzheimer's disease and mild cognitive impairment revealed by Regional Homogeneity. *NeuroImage* (2012).
117. Kjaer, T. W. *et al.* Increased dopamine tone during meditation-induced change of consciousness. *Cognitive Brain Research* (2002).
118. Lazar, S. W. *et al.* Functional brain mapping of the relaxation response and meditation. *NeuroReport* (2000).

119. Tang, Y. Y. *et al.* Central and autonomic nervous system interaction is altered by short-term meditation. *Proceedings of the National Academy of Sciences of the United States of America* (2009).
120. Libby, D. J., Worhunsky, P. D., Pilver, C. E. & Brewer, J. A. Meditation-induced changes in high-frequency heart rate variability predict smoking outcomes. *Frontiers in Human Neuroscience* (2012).
121. Afonso, R. F. *et al.* Greater cortical thickness in elderly female yoga practitioners-A cross-sectional study. *Frontiers in Aging Neuroscience* (2017).
122. Creswell, J. D. *et al.* Alterations in resting-state functional connectivity link mindfulness meditation with reduced interleukin-6: A randomized controlled trial. *Biological Psychiatry* **80**, 53–61 (2016).
123. Froeliger, B. *et al.* Meditation-state functional connectivity (msFC): Strengthening of the dorsal attention network and beyond. *Evidence-based Complementary and Alternative Medicine* (2012).
124. Hasenkamp, W. & Barsalou, L. W. Effects of Meditation Experience on Functional Connectivity of Distributed Brain Networks. *Frontiers in Human Neuroscience* **6** (2012).
125. Chen, V. C.-H. *et al.* Assessment of brain functional connectome alternations and correlation with depression and anxiety in major depressive disorders. *PeerJ* **5**, e3147 (2017).
126. Wang, L. *et al.* Amplitude of Low-Frequency Oscillations in First-Episode, Treatment-Naive Patients with Major Depressive Disorder: A Resting-State Functional MRI Study. *PLoS ONE* **7**, 1–10 (2012).
127. Xu, Z. *et al.* Altered resting-state brain activities in drug-naïve major depressive disorder assessed by fMRI: Associations with somatic symptoms defined by Yin-Yang theory of the traditional Chinese Medicine. *Frontiers in Psychiatry* **9**, 1–10 (2018).
128. Herwig, U., Kaffenberger, T., Jäncke, L. & Brühl, A. B. Self-related awareness and emotion regulation. *NeuroImage* **50**, 734–741 (2010).
129. Lutz, J. *et al.* Altered processing of self-related emotional stimuli in mindfulness meditators. *NeuroImage* **124**, 958–967 (2016).
130. Garrison, K. A., Scheinost, D., Constable, R. T. & Brewer, J. A. BOLD signal and functional connectivity associated with loving kindness meditation. *Brain and Behavior* **4**, 337–347 (2014).

131. Shao, R., Keuper, K., Geng, X. & Lee, T. M. Pons to Posterior Cingulate Functional Projections Predict Affective Processing Changes in the Elderly Following Eight Weeks of Meditation Training. *EBioMedicine* **10**, 236–248 (2016).
132. Grant, J. A., Courtemanche, J., Duerden, E. G., Duncan, G. H. & Rainville, P. Cortical Thickness and Pain Sensitivity in Zen Meditators. *Emotion* **10**, 43–53 (2010).
133. Li, G. Resting-state functional changes in the precuneus within first-episode drug-naïve patients with MDD. *Neuropsychiatric Disease and Treatment*, 1991–1998 (2018).
134. Peng, D. *et al.* Dissociated large-scale functional connectivity networks of the precuneus in medication-naïve first-episode depression. *Psychiatry Research - Neuroimaging* (2015).
135. Marchand, W. R. *Mindfulness-based stress reduction, mindfulness-based cognitive therapy, and zen meditation for depression, anxiety, pain, and psychological distress* 2012.
136. Dickenson, J., Berkman, E. T., Arch, J. & Lieberman, M. D. Neural correlates of focused attention during a brief mindfulness induction. *Social Cognitive and Affective Neuroscience* (2013).
137. Bærentsen, K. B. *et al.* An investigation of brain processes supporting meditation. *Cognitive Processing* **11**, 57–84 (2010).
138. Chang, C. *et al.* Association between heart rate variability and fluctuations in resting-state functional connectivity. *NeuroImage* (2013).

## PUBLIKATIONSLISTE

**Yang, C.**, Barrós-Loscertales, A., Li, M., Pinazo, D., Borchardt, V., Ávila, C., and Walter, M. Alterations in Brain Structure and Amplitude of Low-frequency after 8 weeks of Mindfulness Meditation Training in Meditation-Naïve Subjects. *Sci Rep* 9, 10977 (2019) doi:10.1155/2016/9504642.

**Yang, C.**, Barrós-Loscertales, A., Pinazo, D., Ventura-Campos, N., Borchardt, V., Bustamante, J.C., Rodríguez-Pujadas, A., Fuentes-Claramonte, P., Balaguer, R., Ávila, C., and Walter, M. State and Training Effects of Mindfulness Meditation on Brain Networks Reflect Neuronal Mechanisms of Its Antidepressant Effect, *Neural Plasticity*, vol. 2016, Article ID 9504642, 14 pages, (2016) doi:10.1038/s41598-019-47470-4

## ERKLÄRUNG ZUR STRAFRECHTLICHEN VERURTEILUNG

Ich erkläre hiermit, nicht wegen einer Straftat verurteilt worden zu sein, die Wissenschafts-  
bezug hat.



Magdeburg, den 28.11.2019

---

## EHRENERKLÄRUNG

Ich versichere hiermit, dass ich die vorliegende Arbeit ohne unzulässige Hilfe Dritter und ohne Benutzung anderer als der angegebenen Hilfsmittel angefertigt habe; verwendete fremde und eigene Quellen sind als solche kenntlich gemacht. Ich habe insbesondere nicht wissentlich: Ergebnisse erfunden oder widersprüchlich Ergebnisse verschwiegen, statistische Verfahren absichtlich missbraucht, um Daten in ungerechtfertigter Weise zu interpretieren, fremde Ergebnisse oder Veröffentlichungen plagiiert, fremde Forschungsergebnisse verzerrt wiedergegeben.

Mir ist bekannt, dass Verste gegen das Urheberrecht Unterlassungs- und Schadensersatzansprüche des Urhebers sowie eine strafrechtliche Ahndung durch die Strafverfolgungsbehörden begründen kann.

Ich erkläre mich damit einverstanden, dass die Arbeit ggf. mit Mitteln der elektronischen Datenverarbeitung auf Plagiate überprüft werden kann. Die Arbeit wurde bisher weder im Inland noch im Ausland in gleicher oder ähnlicher Form als Dissertation eingereicht und ist als Ganzes auch noch nicht veröffentlicht.



Magdeburg, den 28.11.2019